

Resonant scattering of electrons by molecules

To cite this article: J N Bardsley and F Mandl 1968 *Rep. Prog. Phys.* **31** 471

View the [article online](#) for updates and enhancements.

You may also like

- [Powers of the Vandermonde determinant, Schur functions and recursive formulas](#)
C Ballantine
- [Detection and analysis of the \$1P^0\$ and \$3P^0\$ 'shape' resonances of \$H^+\$ using stabilization](#)
M Cortes, A Macias, F Martin et al.
- [Asymptotic model for shape resonance control of diatomics by intense non-resonant light: universality in the single-channel approximation](#)
Anne Crubellier, Rosario González-Férez, Christiane P Koch et al.

Resonant scattering of electrons by molecules

J. N. BARDSLEY AND F. MANDL

Department of Theoretical Physics, University of Manchester

Contents

	Page
1. Introduction	472
I. The structure of resonances	
2. The classification of resonances in molecules	473
2.1. Shape resonances	474
2.2. Electron-excited Feshbach resonances	475
2.3. Nuclear-excited Feshbach resonances	475
3. Shape resonances	476
3.1. The 3 ev resonance of H_2^-	477
3.2. The 2 ev resonance of N_2^-	478
3.3. The 1.75 ev resonance of CO^-	479
3.4. The 1.2 ev resonance of $C_6H_6^-$	479
4. Electron-excited Feshbach resonances	480
4.1. Dissociative recombination in H_2^+	481
4.2. Dissociative recombination in NO^+	482
4.3. The 12 ev resonances of H_2^-	483
5. Nuclear-excited Feshbach resonances	484
5.1. The electronic ground state of O_2^-	484
5.2. Rydberg states of neutral molecules	484
5.3. Large molecules	485
5.4. Polar molecules	485
6. Further examples of resonances	486
6.1. The 10 ev resonance of H_2^-	486
6.2. The transmission peaks in NO and O_2	488
6.3. The 11.5 ev resonance of N_2^-	489
6.4. The low-energy resonances of $C_2H_4^-$	491
II. Collision processes	
7. Resonance formalisms	492
7.1. The theories of Siegert, and of Kapur and Peierls	492
7.2. The projection operator formalism of Feshbach	493
7.3. The configuration interaction theory of Fano	495
8. Definition of molecular resonances	497
9. The nuclear wave equation	500
9.1. Derivation of the nuclear wave equation	500
9.2. Solution of the nuclear wave equation	503
10. Dissociative attachment	504
10.1. The cross section for dissociative attachment	504
10.2. Dissociative attachment in H_2 at low energies	507
10.3. Dissociative attachment in H_2 near 10 ev	507
10.4. Dissociative attachment in hot O_2	509
10.5. Dissociative attachment in methane	510
10.6. Dissociative attachment in other molecules	511
11. Vibrational excitation	511
11.1. Theory of vibrational excitation	511

	Page
11.2. Elastic scattering	514
11.3. Vibrational excitation of H ₂ at low energies	515
11.4. Electron scattering by H ₂ near 12 eV	516
11.5. Electron scattering by N ₂ near 2 eV	519
12. Non-adiabatic collision processes	521
12.1. Vibrationally excited Rydberg states	521
12.2. Long-lived resonances in polyatomic molecules	522
13. Heavy particle collisions	523
13.1. Electron detachment in H-H ⁻ collisions	523
13.2. Associative detachment in H-H ⁻ collisions at thermal energies	524
13.3. Ionization in the collisions of two neutral atoms	526
13.4. Electronically stable resonances	527
14. Conclusions	528
References	528

Abstract. In this article the effect of resonances (i.e. metastable states capable of decaying by electron emission) on electron-molecule and heavy particle collisions is considered. In part I resonances are classified into different types: shape resonances, and electron-excited and nuclear-excited Feshbach resonances. Many of the observed resonances and their properties are discussed in terms of this classification. In part II resonance scattering theory is summarized. A survey is given of experiments, and their theoretical analysis, on resonance phenomena in processes such as vibrational excitation and dissociative attachment of molecules by electron impact and electron detachment in atom-atom collisions.

1. Introduction

In this article we shall discuss resonances in molecules and molecular ions, that is states in which an electron is temporarily retained by a molecular system. Such a resonance is not a true bound, i.e. stationary, state but is a temporary state capable of decaying by electron emission. In collision processes the formation of a resonance from the target and projectile will show up since it generally leads to a severe distortion of the projectile wave function. This will be the case provided the lifetime τ of the resonance is long compared with the time the projectile takes to traverse the target. There are different mechanisms for retaining a projectile electron in the target which produce very different characteristic features in scattering experiments. Many of these features have been observed. We shall survey these experiments and their theoretical interpretation in such a way as to facilitate the understanding of similar situations.

Resonances in atoms have recently been reviewed by Burke (1965) and Smith (1966). In molecules a whole wealth of new features arise owing to the motion of the nuclei. In particular there can now be an exchange of energy between electronic and nuclear motion which shows up in elastic scattering and in inelastic processes such as vibrational excitation. The comparatively long lifetime of a resonance will lead to severe distortion of the nuclear motion and greatly enhanced inelastic cross sections. Another new feature results from the possibility of the molecular resonance complex dissociating, and this process will occur in competition with autoionization, i.e. the re-emission of the electron. These features will also show up in the inverse processes of atom-atom and atom-ion collisions.

The basic physical property of molecules is the large ratio of nuclear to electronic masses. This leads to nuclear velocities being very slow compared with electronic velocities. This is the basis of the Born–Oppenheimer separation of electronic and nuclear motions. A modification of this approach also leads to a wave equation for the nuclear motion in an electronic resonant state. This equation allows for the decay of the resonance in which the nuclei move and, in the case of electron scattering, for the formation of the resonance through electron capture by the target.

In part I of this article we shall discuss the different types of resonance mechanisms in detail and give examples of such resonances. In atoms one has shape resonances (where the projectile is retained in the ground state or an excited state of the target by a potential barrier) and electron-excited Feshbach resonances (where the projectile loses energy in electronic excitation of the target and is left with insufficient energy to escape). In molecules there exists the new possibility of a nuclear-excited Feshbach resonance, i.e. the electron excites the nuclear instead of the electronic degrees of freedom of the target.

All these types of resonances occur as intermediate states in collision processes, and most of the information about resonances has been derived from an analysis of scattering experiments. Typical processes are

(i) elastic or inelastic scattering



(ii) dissociative attachment or recombination



(iii) atom–negative-ion collisions such as



or



and so on.

What all these processes have in common is that they occur via an intermediate complex which can autoionize. There may also be other decay modes. The interesting situations are precisely those where competition occurs between such different modes.

In part II of this article we shall study resonant collision processes. We shall mainly be concerned with diatomic molecules for which most theoretical work has been done. After a review of the several formalisms which have been applied to molecules, we shall consider particular collision experiments and their theoretical analysis.

I. The structure of resonances

2. The classification of resonances in molecules

As was stated in the introduction, a resonant state Ψ_n^* can be regarded as a temporary bound state of the projectile and target, capable of decaying by electron

emission. It will therefore have a time dependence

$$\Psi_n \propto \exp\left(-iW_n \frac{t}{\hbar}\right) \quad (2.1)$$

with a complex energy

$$W_n \equiv E_n - \frac{1}{2}i\Gamma_n. \quad (2.2)$$

It follows that

$$|\Psi_n|^2 \propto \exp\left(-\Gamma_n \frac{t}{\hbar}\right) \quad (2.3)$$

i.e. the state Ψ_n decays with a lifetime $\tau = \hbar/\Gamma_n$. Γ_n is called the width of the resonance.

For a resonance to occur there must be some mechanism for binding the electron temporarily to the target. Thus we can classify resonances according to the means by which the projectile is trapped.

2.1. Shape resonances

The simplest trapping mechanism is a potential barrier. Let us suppose that the incident particle experiences a region of attractive potential surrounded by a region of repulsive potential. If the particle enters the region of attractive potential its escape will be hindered by the potential barrier surrounding it. Resonances which are supported by potential barriers will be called shape resonances. The best-known examples are the radioactive nuclei which decay by the emission of an α particle which has tunneled through the Coulomb barrier.

For simplicity we shall consider resonances occurring in the collisions of electrons with diatomic molecules. The target states will be expressed as products of electronic wave functions $\chi_\nu(q, \mathbf{R})$ and nuclear functions $\zeta_\nu(\mathbf{R})$ (q denotes the coordinates of all the target electrons and \mathbf{R} the internuclear position vector). The energy of each target state will be denoted by ϵ_ν . If the coordinates of the incident electron are represented by \mathbf{r} the resonant wave function $\Psi_n(\mathbf{r}, q, \mathbf{R})$ can then be expressed in a close-coupling expansion:

$$\Psi_n(\mathbf{r}, q, \mathbf{R}) = \sum_\nu \chi_\nu(q, \mathbf{R}) \zeta_\nu(\mathbf{R}) f_{n\nu}(\mathbf{r}). \quad (2.4)$$

Throughout the article ν will be used as a collective index to denote any or all of the quantum numbers of the system.

In the simplest shape resonances the electronic motion of the target is affected little by the presence of the incident particle. In this case the expansion (2.4) is dominated by the terms involving the ground electronic state $\chi_0(q, \mathbf{R})$. An example of such a resonance is the 3 eV resonance of H_2^- . This has the structure of the ground state of H_2 together with an electron in the orbital ($2p\sigma_u$) (see §3.1).

There are other shape resonances in which the wave function (2.4) is dominated by the terms corresponding to an excited electronic target state. In these the incident electron excites a target state whose energy is less than the resonant energy. The extra electron has sufficient energy to escape from the target leaving it in its excited state. If the potential experienced by the electron as it is moving in the field of the excited target contains a barrier then its escape will be hindered and the electron will become temporarily bound to the target. The simplest example of

these core-excited shape resonances is the $1P$ state of H^- at 10.22 eV (Macek and Burke 1967). Its wave function has two dominant terms, one corresponding to the target electron being in the $2s$ state and the other with the target electron in the $2p$ state. The $2s$ and $2p$ states of H are degenerate at an energy 0.018 eV *below* the energy of the resonance.

The characteristic of shape resonances is that the wave functions are dominated by the open-channel components. In the expansion (2.4) the important terms are those corresponding to target states with energies less than the resonant energy. This means that shape resonances are often broad, but there are narrow ones (the H^- resonance quoted above has a width of 0.015 eV).

2.2. Electron-excited Feshbach resonances

Feshbach resonances occur when the incident electron loses energy in exciting the target and finds itself with insufficient energy to escape while the target remains in its excited state. Before the electron can be emitted it must reabsorb energy from the target.

The simplest situation would be that the incident electron excites only a single electronic target state $\chi_v(q, \mathbf{R})$ for which the vibrational levels ϵ_v lie above the resonant energy. In this case the expansion (2.4) would be dominated by the terms containing this electronic state $\chi_v(q, \mathbf{R})$. In the more general case several electronic states of the target may be important, but for a Feshbach resonance it must be closed-channel components which predominate.

The fact that the open-channel components are small means that the resonance is narrow. Thus Feshbach resonances are nearly always narrow although for large nuclear separations some become broad (see § 6.1). The wave functions for narrow Feshbach resonances can be approximated by the removal of the open-channel components which turns them into bound states.

Feshbach resonances in molecules can be divided into two types, depending on whether the kinetic energy of the incident electron is absorbed into the electronic or nuclear motion. The two types will be treated separately since they often reveal themselves in different processes.

Examples of Feshbach resonances in which electronic excitation occurs are the two resonances occurring in $e-H_2$ collisions at about 12 eV. These and other examples will be discussed in § 4.

2.3. Nuclear-excited Feshbach resonances

These are Feshbach resonances in which the kinetic energy of the incident electron is absorbed solely into the nuclear motion of the target. The collision does not involve excitation of the electronic motion in the target.

The previous two types of resonance can be discussed within the Born-Oppenheimer separation of nuclear and electronic motion. In this third type the resonances are formed by an interchange of energy between these two modes, and thus the existence of the resonance is a consequence of the breakdown of the Born-Oppenheimer approximation. Thus inclusion of the nuclear motion is essential to the definition of these resonances. If the nuclei were kept fixed the resonances would become stable against electron emission.

The situation can be illustrated by means of figure 1. This shows the potential curves for a molecule XY^- and for the ground state of the corresponding neutral molecule XY . It will be seen that the ground vibrational state of XY^- is a bound state. However, its excited vibrational levels are above the ground state of XY . Thus, for example, the first excited vibrational level of XY^- can be formed temporarily in the collision of electrons of energy ϵ_{10} with molecules XY in their vibrational ground state. This resonant state will decay by the emission of electrons of the same energy and the target will revert to its original state.

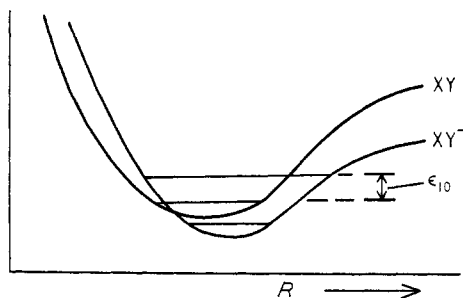


Figure 1. The potential energy curves for the ground states of the molecules XY and XY^- . The excited vibrational levels of XY^- will act as resonances in e - XY scattering.

The resonances of this type which have received most attention from both theoreticians and experimenters are the vibrationally excited Rydberg states with high principal quantum number. For values of this quantum number greater than 7 almost all the vibrationally excited levels lie above the energy of the ground state of the corresponding positive ion (see §§ 5.2 and 12.1). For principal quantum numbers of the order of 30 or more even the rotationally excited levels of the lowest vibrational state will be unstable against electron emission.

3. Shape resonances

We have already stated that shape resonances occur when the incident particle experiences a region of attractive potential surrounded by a repulsive potential barrier. This is illustrated in figure 2. The energy E_n at which the resonance occurs is determined mainly by the depth V_{\min} and the extent of the attractive potential. On the other hand, the resonant width is determined by the height $V_{\max} - E_n$ of the barrier above the resonant energy and by the size $r_2 - r_1$ of the region in which the potential is greater than this energy. This is clear if one remembers that the width is directly proportional to the rate at which the particle escapes by tunnelling through the potential barrier.

It is of interest to consider the effect on a shape resonance of a variation in the depth V_{\min} of the inner region of attractive potential. As this depth is increased, the energy level of the resonance is lowered. As a consequence of the lowering of the energy the particle finds it harder to penetrate through the barrier so that the width becomes smaller. As the energy of the resonance tends to zero, so does the width. If the depth of the attractive potential is increased further the energy of the resonance

becomes negative, escape of the particle is then impossible and so the resonance is turned into a bound state. Thus, although shape resonances are normally broad, it is possible that the width can be very small if the energy available to the escaping electron is small compared with the barrier height. This is illustrated by the 10.22 eV 1P resonance of H^- mentioned in §2.1. This has a width of only 0.015 eV and the kinetic energy of the emitted electron is 0.018 eV.

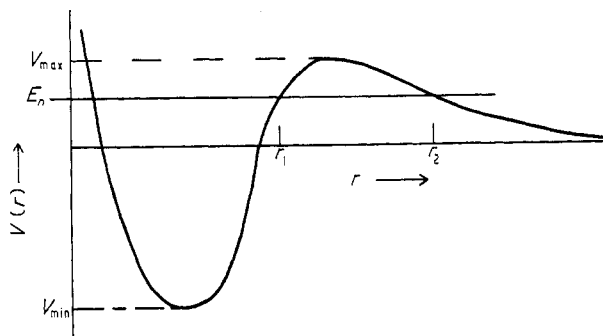


Figure 2. A typical potential capable of supporting a shape resonance. The real part of the resonant energy is E_n . The region of the effective barrier extends from r_1 to r_2 .

The potential necessary for the existence of shape resonances can be found in both nuclear and molecular systems. In nuclear physics the attractive potential is due to the short-range nuclear forces, and the potential barrier is produced by the Coulomb repulsion between protons and by the centrifugal force. In atomic and molecular systems the attractive potential is due to the Coulomb attraction of electrons and protons, whereas the barrier is normally caused by the centrifugal force.

The centrifugal force produces barriers which are of the order of several volts high with thicknesses of a few Bohr radii. Thus narrow shape resonances in which the target is not excited electronically will normally be found at low energies, say between 0 and 5 eV. For the existence of a state with such an energy the short-range attractive potential must be strong enough that it can almost, but not quite, support a bound state. Thus in order to find shape resonances one should examine those molecules which do not have a stable negative ion and in which the lowest unfilled orbital has non-zero angular momentum.

3.1. The 3 eV resonance of H_2^-

The simplest molecule which meets these two conditions is hydrogen, for which the lowest unfilled orbital is ($2p\sigma_u$). In escaping from this orbital an electron from H_2^- must tunnel through a p-wave centrifugal barrier. This barrier has a maximum height of about 5 eV and so can prevent the escape for a very short time only. By using a variational method which will be mentioned in §8, Bardsley *et al.* (1966 a) have shown that at small nuclear separations the ground state of H_2^- is indeed a shape resonance with a lifetime of about 10^{-16} s.

For shape resonances and electron-excited Feshbach resonances the essential properties of a resonance can be indicated by giving its energy and width at each

internuclear distance. The calculated potential energy curve for the H_2^- state is shown in figure 3. Also shown is the potential curve for the ground state of H_2 calculated by the variational method using a wave function of similar complexity to those used to describe the resonant state. The H_2^- state was found to be unstable for nuclear separation less than 2.9 Bohr radii. The calculated width, shown in figure 4, is of the order of a few eV. We suggest that this is typical for p-wave shape resonances.

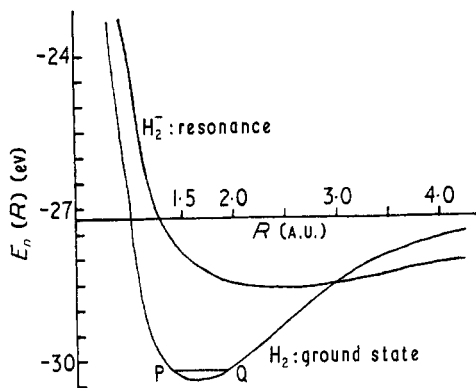


Figure 3. The potential energy curves of the $(1s\sigma_g)^2(2p\sigma_u)^2{}^2\Sigma_u^+$ resonance of H_2^- and of the H_2 ground state calculated with wave functions of similar complexity. The line PQ marks the Franck-Condon region. R is the internuclear distance. (From Bardsley *et al.* 1966 a.)

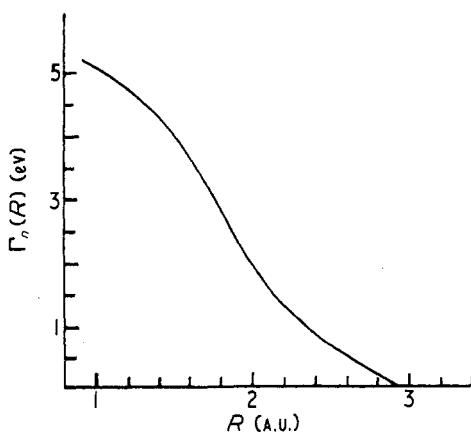


Figure 4. The width of the $(1s\sigma_g)^2(2p\sigma_u)^2{}^2\Sigma_u^+$ resonance of H_2^- . R is the internuclear distance. (From Bardsley *et al.* 1966 a.)

Eliezer *et al.* (1967) have carried out a further variational calculation on this state using a much more flexible trial wave function. However, the variational method which they use gives only the real part of the energy and not the resonant width. Their aim is to calculate a wave function of bound-state form which most closely resembles the true resonant state. However, for such a wide resonance as this, it is likely that allowance for the decay of the resonance will cause a considerable shift in the real part of the energy as well as producing the resonant width.

The effects of this resonance have been observed in vibrational excitation (see § 11.3) and dissociative attachment (see § 10.2). It also causes electron detachment in H-H collisions (see § 13).

3.2. The 2 eV resonance of N_2^-

Considerable structure has been observed in the scattering of low-energy electrons by N_2 . Analysis of the experimental data has shown the structure to be due to a single resonance near 2 eV with a width of between 0.15 and 0.2 eV (see § 11.5). Gilmore (1965) suggested that this may be a shape resonance with the

configuration of the ground state of N_2^- , namely

$$(1s\sigma_g)^2(2p\sigma_u)^2(2s\sigma_g)^2(3p\sigma_u)^2(3s\sigma_g)^2(2p\pi_u)^4(3d\pi_g)^2\Pi_g. \quad (3.1)$$

This configuration is formed by adding the $(3d\pi_g)$ orbital to the ground state of N_2 .

The barrier supporting this resonance arises from the d-wave centrifugal force. Bardsley *et al.* (1967) have constructed a model to represent this barrier and have shown that a width of about 0.2 eV is reasonable for a d-wave shape resonance at 2 eV. The very different values for the width of the low-energy H_2^- and N_2^- resonances can thus be ascribed to the different probabilities of electron penetration through the p-wave and d-wave barriers.

Further confirmation of Gilmore's identification of this resonance has been obtained by Ehrhardt and Willman (1967) who have measured the angular distribution of inelastically scattered electrons. Their results are just as one would expect for a shape resonance with the extra electron in a π_g orbital (see §11.5, figure 26).

3.3. The 1.75 eV resonance of CO^-

A low-energy resonance has also been observed in electron scattering by CO at an energy close to 1.75 eV (see §11.5). Since CO is isoelectronic with N_2 it is natural to ascribe the resonance to the configuration (3.1). However, there is one difference between the two molecules. The CO molecule is not symmetric with respect to inversion, so that the g-u symmetry is no longer valid. This means that the $3d\pi$ orbital contains p-wave components. The effect of these p-wave components on the scattering cross sections will be discussed in §11.5.

3.4. The 1.2 eV resonance of $C_6H_6^-$

This example shows that shape resonances are not confined to diatomic molecules. By studying inelastic electron scattering by a scavenger technique Compton *et al.* (1966 a) observed resonances near 1 eV in benzene and six of its derivatives. Boness *et al.* (1967) also studied the benzene resonance by passing a beam of electrons through benzene and measuring the transmitted current. After removing the background current they obtained the results shown in figure 5. It will be seen from this figure that some of the vibrational structure of the resonance has been resolved, so that the resonance must be narrow with a width not exceeding 0.05 eV.

Let us therefore consider the structure of the ground state of $C_6H_6^-$ to see if this narrow width can be explained. The neutral benzene molecule has 42 electrons. Twelve of these are localized in 1s orbitals of the carbon atoms. Twenty-four electrons are in ' σ orbitals' which extend over all the atoms in the molecules. The remaining six electrons are in ' π orbitals' which are shared between the carbon atoms. These π orbitals have the form of linear combinations of 2p orbitals of the carbon atoms, each directed normally to the plane of the molecule. If these atomic orbitals are indicated by p_α , the π orbitals can be expressed as

$$\psi = \sum_{\alpha=1}^6 c_\alpha p_\alpha.$$

Because of the sixfold axis of symmetry the coefficients c_α must take the values $\exp(im\alpha\pi/3)$. There are six π orbitals with $m = 0, \pm 1, \pm 2, 3$. In the neutral molecule C_6H_6 three of these orbitals are fully occupied. These have $m = 0$ and ± 1 . The ground state of $C_6H_6^-$ will be formed by adding an electron in a π orbital with $|m| = 2$.

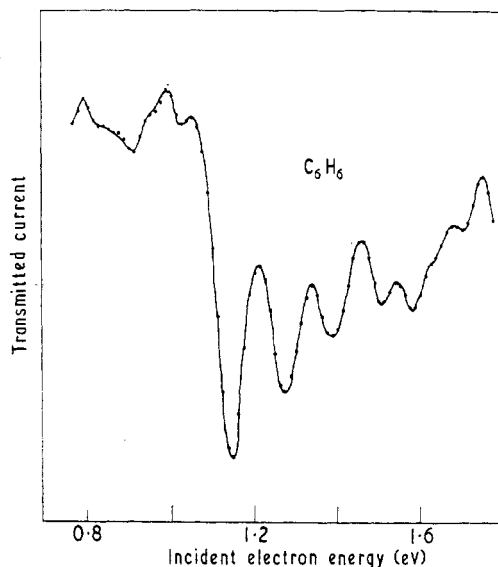


Figure 5. The transmitted current for electrons passed through benzene. (From Boness *et al.* 1967.)

Thus the extra electron in the $C_6H_6^-$ ground state has angular momentum 2 about the axis of symmetry. The parity of the extra orbital is odd; hence if its wave function is expanded in spherical harmonics the first term will have $l = 3$. Thus the resonance is supported by an f-wave barrier. Penetration of an electron through this barrier would be very difficult and it seems probable that the width is even less than 0.05 eV.

It seems that the determination of the width of this resonance will demand the use of electron beams with very high resolution. A useful experiment which should be within the scope of present equipment is the measurement of the angular distribution of inelastically scattered electrons. This would test whether the scattering is indeed dominated by the f-wave components.

4. Electron-excited Feshbach resonances

In these resonances the incident electron becomes bound to an electronically excited state of the target. Most of the resonances which have been observed in atomic systems are of this type. They also play an important role in electron collisions with both neutral and positively charged molecules. The resonances in electron-ion scattering are of particular interest since they lead to dissociative

recombination. The recombination process can be represented as



i.e. it occurs through the formation and subsequent dissociation of molecular resonant states XY^* (Bates 1950, Nielsen and Dahler 1966, Bardsley 1968 b).

The potential energy curves necessary for recombination to occur are shown in figure 6. Since the electron-ion collisions involve thermal electrons, the curve XY must cross over that of the ionic ground state XY^+ near to the equilibrium separation of the latter. Unless this is the case the probability of resonance formation in thermal collisions will be very small. Secondly, the dissociation limit of XY^* must be less than the ground-state energy of XY^+ , in order that the molecule should dissociate after the formation of the resonant state.

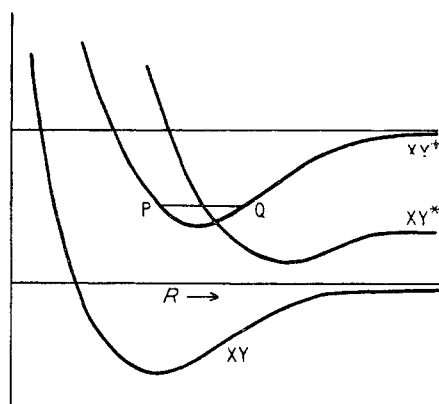


Figure 6. Potential energy curves for dissociative recombination. The line PQ marks the Franck-Condon region of the XY^+ ion.

There are two problems in the calculation of the rates of dissociative recombination. Firstly, the potential energy curves of suitable resonant states XY^* must be determined and, secondly, the rate of resonance formation must be found. The latter problem is equivalent to the calculation of the widths of the resonant states. Two methods have been proposed for tackling these problems, and we shall give two examples which illustrate these methods.

4.1. Dissociative recombination in H_2^+

It is feasible that *a priori* calculations will soon be made of the rate of the recombination of electrons with H_2^+ ions. The determination both of the potential energy curves and the widths of the appropriate states should be within the capacity of present computational techniques.

The dominant configurations of electron-excited Feshbach resonances in H_2 must have both electrons in excited orbitals. The resonant states whose potential curves are most likely to be suitable for recombination are those for which both electrons are in the $(2s\sigma_g)$, $(2p\sigma_u)$ or $(2p\pi_u)$ orbitals. Three of the states which can be formed in this manner have already been investigated using perturbation theory.

These are

$$(2p\sigma_u)(2p\pi_u) \ ^3\Pi_g \quad (4.2)$$

$$(2p\sigma_u)(2s\sigma_g) \ ^3\Sigma_u^+ \quad (4.3)$$

$$(2p\sigma_u)^2 \ ^1\Sigma_g^+ \quad (4.4)$$

The first two of these states were studied by Bauer and Wu (1956). They used perturbation theory both in the determination of the potential curves and in the calculation of the resonant formation cross section. Unfortunately, they used plane waves to describe the initial electron-ion scattering wave function, and the cross sections they obtain for the state (4.2) show an energy dependence far from that expected (Bardsley 1968 a). The results for state (4.3) seem much better and calculations using Coulomb wave functions by Wilkins (1966) have given similar numbers. Wilkins estimated the contribution of this state to the recombination rate to be $3 \times 10^{-8} \text{ cm}^3 \text{ s}^{-1}$ at 300°K . The resonant state (4.4) has also been studied in perturbation theory by Dubrovsky *et al.* (1967). They predict the contribution of the state to the recombination rate at 300°K to be $2 \times 10^{-8} \text{ cm}^3 \text{ s}^{-1}$.

The rate of recombination in hydrogen has been measured by Popov and Afanaseva (1960) to be $3 \times 10^{-8} \text{ cm}^3 \text{ s}^{-1}$. An earlier experiment by Persson and Brown (1955) had established this value as an upper limit to the recombination rate. Since the nature of the ions involved is not certain (they may be H_3^+ ions) one can only conclude that the rate of recombination of H_2^+ ions does not exceed $3 \times 10^{-8} \text{ cm}^3 \text{ s}^{-1}$. However, there is already a minor disagreement between theory and experiment in that the estimated contribution of two resonances exceeds the observed upper limit for the recombination rate.

The most crucial part of the calculation of the recombination rate lies in the determination of the resonant potential curves. In this respect the methods so far used do not seem to be sufficiently accurate for the present results to be regarded as reliable.

4.2. Dissociative recombination in NO^+

The gases in which large rates of dissociative recombination have been observed are the atmospheric gases N_2^+ , NO^+ , O_2^+ , and the rare gases Ne_2^+ , A_2^+ , Kr_2^+ , Xe_2^+ (Oskam and Mittelstadt 1963, Danilov and Ivanov-Kholodnyi 1965). The *a priori* calculation of these rates will be much more difficult than for H_2^+ . The main difficulty will be in the determination of the resonant potential curves with sufficient accuracy. In order to obtain the recombination rate to within 10% it will be necessary to find the cross-over point of the curves XY^+ and XY^* to within 0.01 \AA . An alternative approach has been suggested by Bardsley (1968 b) who showed that spectroscopic evidence could be used in the determination of potential energy curves and also in the estimation of the resonant widths.

The method was illustrated by the example of nitric oxide. The ground state of NO^+ has the following configuration:

$$[(1s\sigma)^2 (2s\sigma)^2 (2p\sigma)^2 (3s\sigma)^2] (3p\sigma)^2 (2p\pi)^4 \ ^1\Sigma^+ \quad (4.5)$$

Electron-excited Feshbach resonances of NO can be formed by the excitation of an electron from any of these orbitals and the addition of the extra electron into an

unfilled orbital. Bardsley suggested that the following two configurations may lead to resonances suitable to cause recombination:

$$[(1s\sigma)^2(2s\sigma)^2(2p\sigma)^2(3s\sigma)^2](3p\sigma)(2p\pi)^4(3p\pi)^2 \quad (4.6)$$

$$[(1s\sigma)^2(2s\sigma)^2(2p\sigma)^2(3s\sigma)^2](3p\sigma)^2(2p\pi)^3(3p\pi)^2. \quad (4.7)$$

The configuration (4.6) leads to two states $1^2\Sigma$ and $B'^2\Delta$ and the configuration (4.7) leads to the states $B^2\Pi$ and $L'^2\Phi$.

Enough spectroscopic evidence has been obtained for the reconstruction of the potential curves of two of these states, $B^2\Pi$ and $B'^2\Delta$. It was found that both curves cross over that of the ground state of NO^+ within the Franck–Condon region of the latter. (We define the Franck–Condon region as the range of nuclear separations between the classical turning points.) It was found also that the spectroscopic data could be used to estimate the resonant widths, and hence to obtain the cross sections for resonance formation. Thus the contribution of these two states to the recombination rate was assessed. The sum of the two contributions was found to be $2.6 \times 10^{-7} \text{ cm}^3 \text{ s}^{-1}$ as compared with the observed values of $(4.6_{-1.3}^{+0.5}) \times 10^{-7} \text{ cm}^3 \text{ s}^{-1}$ of Gunton and Shaw (1965), and $(5 \pm 2) \times 10^{-7} \text{ cm}^3 \text{ s}^{-1}$ of Young and St. John (1966).

4.3. The 12 eV resonances of H_2^-

The elastic and inelastic scattering of electrons by H_2 , HD and D_2 shows a lot of structure around 12 eV (see § 11.4 for a discussion of the experimental results).

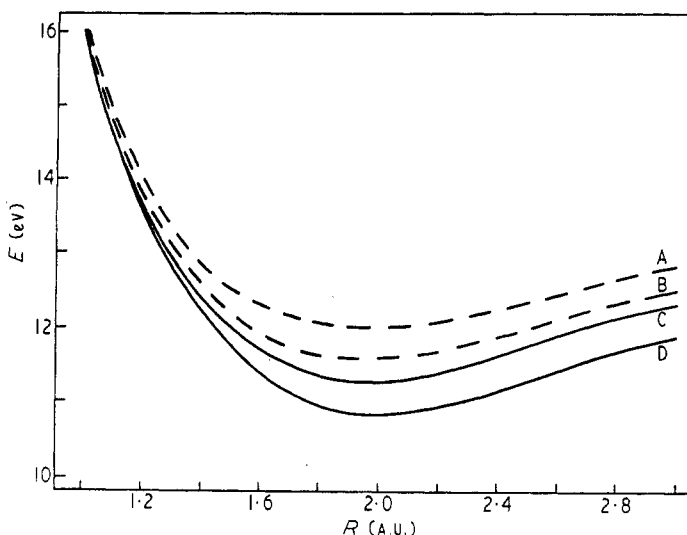


Figure 7. Potential energy curves of the two $2\Sigma_g^+$ resonances of H_2^- and of their parent states. Full curves, H_2^- ; broken curves, H_2 . A, $(1s\sigma_g)(2p\pi_u)c^1\Pi_u$; B, $(1s\sigma_g)(2p\pi_u)c^3\Pi_u$; C, $(c^1\Pi_u)(2p\pi_u)^2\Sigma_g^+$; D, $(c^3\Pi_u)(2p\pi_u)^2\Sigma_g^+$. (From Eliezer *et al.* 1967.)

The structure has been ascribed to the vibrational levels of two electronic resonances. These resonances have been identified by Eliezer *et al.* (1967), who proposed that both have the form

$$(1s\sigma_g)(2p\pi_u)^2 \ 2\Sigma_g^+.$$

The two resonant states differ in the way the electron spins are coupled. One resonance is dominated by the term representing an electron bound to the $(1s\sigma_g)(2p\pi_u)c\ ^3\Pi_u$ state of H_2 , whereas the other represents almost purely an electron bound to the $(1s\sigma_g)(2p\pi_u)c\ ^1\Pi_u$ state. The potential curves of the two resonances and their parent states are shown in figure 7. The fact that both resonant curves lie below the corresponding curves for the parent molecular state demonstrates that these are indeed Feshbach resonances. There is no theoretical evidence concerning the width of these resonances, but the observed cross sections show that the resonances are narrow.

5. Nuclear-excited Feshbach resonances

These resonances have been observed in low-energy electron-molecule scattering and also in the ionization of molecules by electron and photon impact. We shall first discuss a specific example and then describe three groups of these resonances which are of special interest.

5.1. The electronic ground state of O_2^-

This type of resonance is expected to exist in oxygen, since there exists a stable O_2^- ion. Several experiments have studied the formation of this stable O_2^- ion by electron attachment to neutral molecules. This attachment takes place in two stages, involving a Feshbach resonance as an intermediate state. First a low-energy electron collides with a molecule and is trapped through the vibrational excitation of the molecule. Secondly, the excess vibrational energy is lost in a collision with another molecule and the negative ion is stabilized.

Since this is a three-body process, its rate will be dependent upon the gas pressure unless saturation can be achieved, that is unless the pressure is so high that every resonant state is stabilized by a further collision. Bloch and Bradbury (1935) appeared to have achieved saturation but recent experiments (Van Lint *et al.* 1960, Chanin *et al.* 1962) make it seem unlikely that it was accomplished. This is unfortunate since the cross section for resonance formation could be obtained from the experiments if saturation could be reached. Chanin *et al.* attempted to place limits on the resonant width. They estimated the resonant lifetime to be between 10^{-13} and 10^{-10} s. This corresponds to a width between 10^{-2} and 10^{-5} eV.

5.2. Rydberg states of neutral molecules

Associated with every electronic state of molecular positive ions is a series of states of the neutral molecule formed by adding to the ion an electron in a hydrogenic orbital with high principal quantum number. The higher members of these Rydberg series have very small electron affinities and the energy of many of their excited vibrational states will be above the energy of the lowest vibrational level of the corresponding ion. Thus these states will lead to many resonances which may be observed in low-energy electron-ion collisions or in the ionization of neutral molecules just above threshold. The existence of these resonances was used by

Beutler and Junger (1936) in the determination of the ionization potential of hydrogen. References to many more recent ionization experiments are given by Berry (1966). The theory of these resonances will be discussed in §12.1.

Excited rotational levels of Rydberg states may also be unstable against electron emission and so lead to resonances. However, these resonances will only be observed in those members of the Rydberg series for which the energy required to detach an electron is less than (or of the same order as) the rotational spacing. For the case of hydrogen this means that the outermost electron must move in an orbit with principal quantum number of the order of 30 or more. It will be very difficult to observe these resonances in ionization experiments because of the very small probability for excitation of these levels. However, it has been shown by Stabler (1963) that in thermal collisions of electrons with molecular positive ions the cross section for the formation of these resonances should be as high as 10^{-13} or 10^{-14} cm².

Both rotationally excited and vibrationally excited resonant states have been examined as possible intermediate states in dissociative recombination (Stabler 1963, Chen and Mittleman 1967, Bardsley 1968 b). In thermal electron collisions with molecular ions these resonances will be formed and they will have lifetimes varying from 10^{-12} to 10^{-5} s (see §12). If the Rydberg state can be stabilized against electron emission then recombination will take place. Stabler (1963) found that this stabilization could not be achieved by further collisions or by the emission of radiation, but Bardsley (1968 b) has suggested that predissociation may occur sufficiently rapidly for these states to be significant in the recombination. However, for predissociation to occur before electron emission it is necessary that the formation of the resonance should have involved vibrational excitation. These suggestions have yet to be substantiated but, if they are proved to be well founded, it will not be possible to treat dissociative recombination simply as the analogous process to dissociative attachment as will be done in §10.

5.3. Large molecules

The resonances formed by vibrationally excited levels of stable electronic states are of particular interest in large polyatomic molecules. In these the energy which is transferred from the incident electron is distributed among the many vibrational modes of the molecule. A considerable time may then elapse before the excess energy is concentrated again in one mode so that it can be given back to the extra electron. Thus these resonances will have extremely long lifetimes. Compton *et al.* (1966 b) have measured the lifetimes of four of these resonances, in $C_6H_5NO_2^-$, SF_6^- , $(CH_3CO)_2^-$ and $(CHO)_2^-$, to be 40, 25, 12 and 2.5 μ s respectively. The interpretation of these results will be discussed in §12.2.

5.4. Polar molecules

There has been much controversy in recent months about the cause of the high momentum-transfer cross sections observed in thermal collisions of electrons with polar molecules. The cross sections were calculated using the Born approximation by Altshuler (1957), and all the observed cross sections are found to exceed the predictions of the theory, sometimes by factors of 2 or more. Turner (1966) has

pointed out that most of the discrepancies could be caused by the induced polarization of the molecules, but that this could not be so for H_2O , D_2O and H_2S which have small polarizabilities.

Turner suggested that the high cross sections for these cases could be attributed to the formation of temporary negative ions. He assumed that the interaction between the electron and the polar molecule could lead to a bound state with a very small electron affinity. The excited rotational or vibrational levels of the state could then act as resonances in the electron-molecule scattering.

The validity of this proposal clearly depends on the existence of weakly bound states of the electron-molecule system. After the publication of Turner's paper many authors examined the spectrum of electrons moving in the field of a dipole moment. They found that, if the dipole moment exceeds a critical value of 0.64 A.U., there are an infinite number of bound states, whereas for moments below this value there are no bound states (see e.g. Levy-Leblond 1967). This critical value is smaller than the dipole moment of H_2O and D_2O , but larger than that of H_2S .

Contrary to the conclusion of several authors, this fact does not mean that nuclear-excited resonances cannot exist for H_2S . For molecules with small dipole moments there will not be an infinite number of bound electronic states of the negative ion, but the combination of the short-range electrostatic interaction *and* the long-range dipole field may be sufficient to support a single bound state (Crawford 1967).

Thus it is still unclear whether the capture of the incident electron through nuclear excitation is responsible for the high momentum-transfer cross sections. Recent evidence suggesting that nuclear excitation may be involved comes from the observation of Stockdale *et al.* (1967), who show that the cases where the dipole moment is less than or greater than the critical value can be distinguished from the experimental evidence. On the other hand Crawford *et al.* (1967) have pointed out that even without any nuclear excitation it is very likely that the momentum-transfer cross section would be considerably in excess of the predictions of the Born approximation of Altshuler (1957). Support for the latter view has been given by the demonstration by Takayanagi and Itikawa (1968) that the dipole field may give rise to a shape resonance.

6. Further examples of resonances

6.1. The 10 eV resonance of H_2^-

This resonance is of interest because of its role in dissociative attachment in $e-\text{H}_2$ collisions (see §10.3), and in electron detachment in $\text{H}-\text{H}^-$ collisions (see §13.1). In the asymptotic limit of large R the resonance leads to the ground states of H and H^- . Its symmetry is $^2\Sigma_g^+$ and for most internuclear distances the dominant configuration is $(1s\sigma_g)(2p\sigma_u)^2$.

The nature of the resonance can be best described by dividing the complete range of nuclear separations into four regions by introducing the critical values of R_1, R_2, R_3 . The resonant energy and width in the four regions are schematically shown in figure 8.

For $R < R_1$ the resonant energy lies below the energies of all the excited states of H_2 . The resonant wave functions contain only a small component of the H_2

ground state, and so the state is a narrow electron-excited Feshbach resonance. The united atom limit is the 2S resonance of He^- at 19.3 eV which has a width of the order of 0.01 eV (Schulz 1963, Kwok and Mandl 1965).

For $R_1 < R < R_2$ the resonant energy is above that of the $(1s\sigma_g)(2p\sigma_u)^3\Sigma_u^+$ state of H_2 . Since the resonant wave function is dominated by the configuration $(1s\sigma_g)(2p\sigma_u)^2$ the width is large in this region. The only constraint which prevents the electron from immediately escaping, leaving the molecule in the $^3\Sigma_u^+$ state, is the p-wave centrifugal barrier in this channel. Thus for these values of R the state is a core-excited shape resonance.

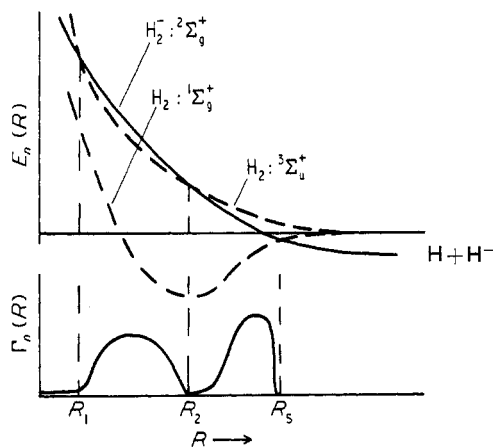


Figure 8. A schematic representation of the potential curve and resonant width for the lowest $^2\Sigma_g^+$ state of H_2^- .

For $R_2 < R < R_3$, the resonant energy is again below that of the $^3\Sigma_u^+$ state of H_2 .† The calculations of Eliezer *et al.* (1967) suggest that $R_2 \approx 1.5$ A.U. If this is so, then for values of R just greater than R_2 the ground-state components in the resonant wave function will still be small and the state will again be a narrow electron-excited Feshbach resonance. However, as R is increased the ground-state components become more important since the asymptotic form of the wave function for large R demands an equal contribution from the ground-state and excited-state components of the wave function (Bardsley *et al.* 1966 a). Hence for the larger values of R within this range the resonance will have a large width, of the order of 1 eV.

For $R > R_3$ the resonant energy is below that of the ground state of H_2 and so the resonance is a bound state.

The potential curve and the width of this resonance were calculated by Bardsley *et al.* (1966 a) using the variational principle mentioned in § 8. The wave functions

† Burke (1968) has pointed out that the opening and closing of the $^3\Sigma_u^+$ channel, as R varies, leads to an interesting mathematical problem. He shows that as a new channel opens or closes one of two things must happen. Either the resonant width must be zero at the critical value of R or else there must be two poles of the S matrix which are important. On physical grounds the second explanation seems most reasonable. The effect on cross sections will probably be small.

used were relatively crude and the resonance was found to be above the ${}^3\Sigma_u^+$ state of H_2 throughout the range of nuclear separations from 1 to 6 A.U. Thus the width was found to be large within this range. For small R the width was dominated by decay to the ${}^3\Sigma_u^+$ state but at large R decay to the ground state was also important. The results are shown in figures 9 and 10. The calculations of Eliezer *et al.* (1967)

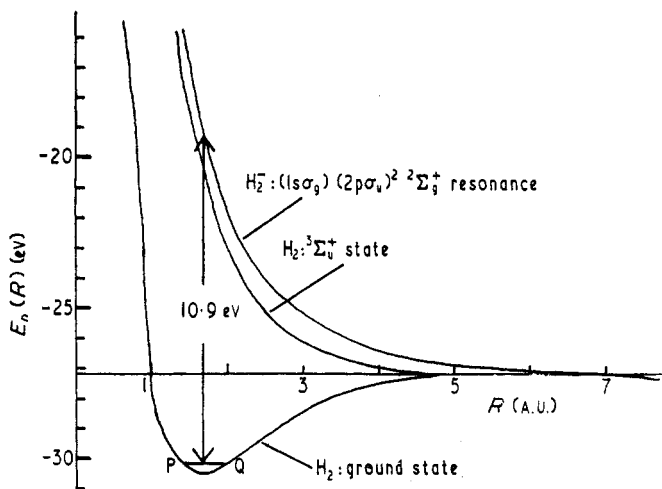


Figure 9. Potential energy curves of the ground (${}^1\Sigma_g^+$) and lowest excited (${}^3\Sigma_u^+$) states of H_2 , and of the $(1s\sigma_g)(2p\sigma_u)^2 {}^2\Sigma_g^+$ resonance of H_2^- . The line PQ marks the Franck-Condon region. (From Bardsley *et al.* 1966 a.)

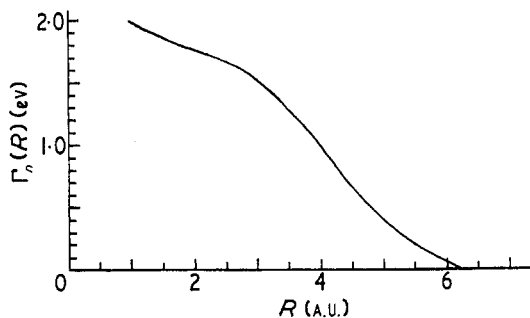


Figure 10. The width of the $(1s\sigma_g)(2p\sigma_u)^2 {}^2\Sigma_g^+$ resonance of H_2^- . (From Bardsley *et al.* 1966 a.)

are shown in figure 11. They used a better wave function but their variational method does not allow for the effects of decay. Thus they do not calculate the resonant width, but the potential curve is probably better than that shown in figure 9.

6.2. The transmission peaks in NO and O_2

Boness and Hasted (1966) have measured the current transmitted by a beam of electrons passing through gases of either NO or O_2 molecules. The results

(figure 12) show a series of peaks between 0.5 and 1.5 eV. Both of these molecules possess a stable negative ion and so the resonances causing these peaks could belong

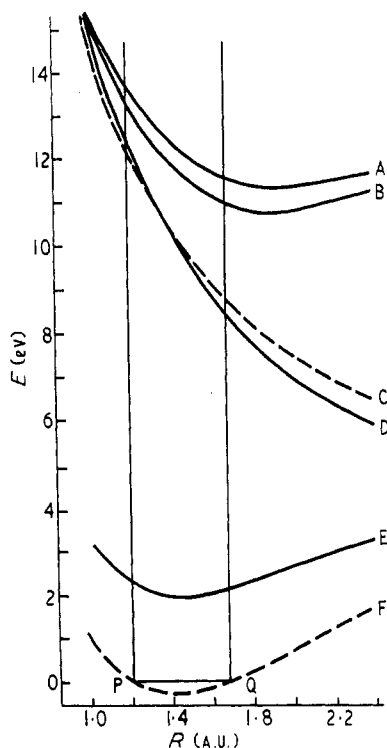


Figure 11. Potential energy curves for H_2^- resonances and some associated H_2 states. Full curves, H_2^- ; broken curves, H_2 . A, $(c^1\Pi_u)(2p\pi_u)^2\Sigma_g^+$; B, $(c^3\Pi_u)(2p\pi_u)^2\Sigma_g^+$; C, $(1s\sigma_g)(2p\sigma_u)^2\Sigma_u^+$; D, $(1s\sigma_g)(2p\sigma_u)^2\Sigma_g^+$; E, $(1s\sigma_g)^2(2p\sigma_u)^2\Sigma_u^+$; F, $x^1\Sigma_g^+$. (From Eliezer *et al.* 1967.)

to any of our three types. It is difficult to decide on theoretical grounds to which type these resonances belong and so more experimental work would be valuable. The most helpful experiment would be the measurement of the angular distribution of inelastically scattered electrons. Estimates of the absolute values of the cross sections and of the widths of the resonant peaks would also be useful.

6.3. The 11.5 eV resonance of N_2^-

The electron transmission experiments of Heideman *et al.* (1966 a) show structure in the transmitted current at energies between 11 and 12 eV, as shown in figure 13. The most obvious feature is a sharp peak at 11.48 ± 0.05 eV. Two additional peaks are seen at 11.75 eV and 11.87 eV. The nature of these resonances has not yet been determined, but Heideman *et al.* suggest that the 11.48 eV peak might be due to an electron-excited Feshbach resonance with an electron bound to a state with a potential curve similar to that of the N_2 ground state. This would explain why a series of several vibrational levels is not seen.

Heideman *et al.* point out that the 11.48 eV peak may be very useful in the calibration of energy scales. They have checked its position against resonances of

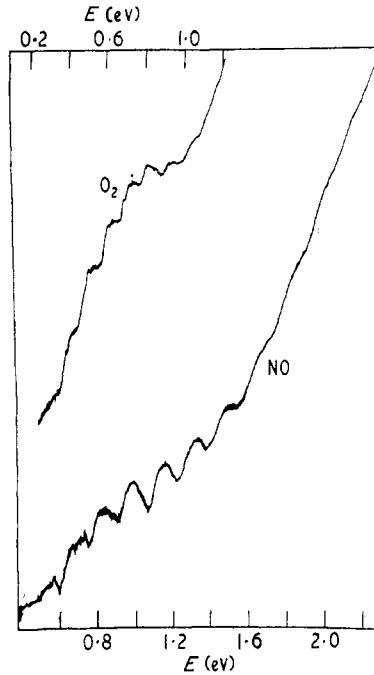


Figure 12. Electron current transmitted through NO and O₂ as function of mean electron energy E (eV). (From Boness and Hasted 1966.)

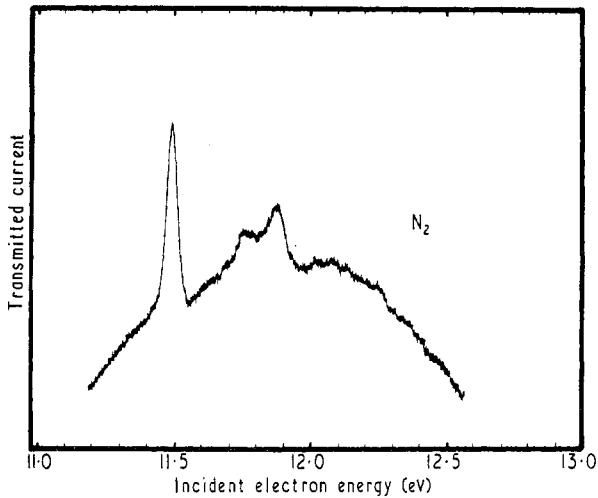


Figure 13. Transmission of electrons by N₂ showing a sharp 'window'-type resonance at 11.48 ± 0.05 eV. (From Heideman *et al.* 1966 a.)

atomic helium and argon and claim an accuracy of 0.05 eV in their determination of its position. The great advantage of using this resonance is that its energy is below

the ionization potential of many gases and this makes it possible to avoid changes in contact potentials caused by ion formation.

6.4. The low-energy resonances of $C_2H_4^-$

Boness *et al.* (1967) have observed two resonances in the transmitted current of electrons in a gas of ethylene, as shown in figure 14. The peaks occur at energies close to 0.2 eV and 1.3 eV, but it is not possible to estimate the resonant widths from their experiment. The upper resonance has also been seen by Bowman and Miller (1965), but at an energy of 1.7 eV.

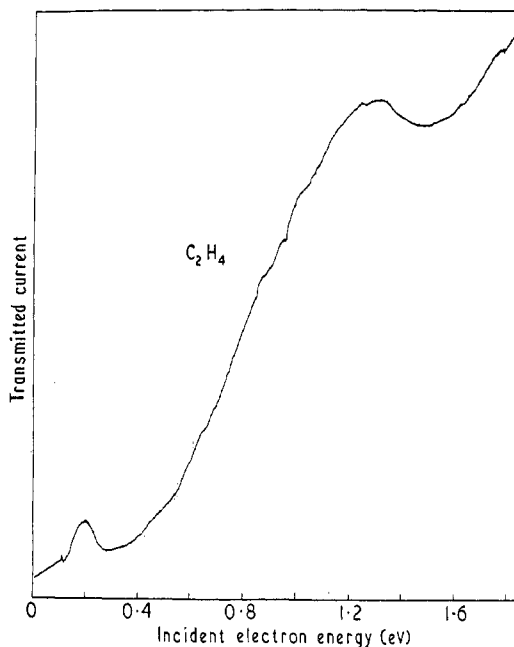


Figure 14. The transmitted current for electrons passed through ethylene. (From Boness *et al.* 1967.)

Ethylene is similar to benzene in that the lowest unfilled orbital is a π orbital. Fourteen of its sixteen electrons are in σ orbitals, which are symmetric with respect to reflection in the plane of the molecule. Of these fourteen electrons, four are localized near the carbon nuclei, and the other ten are shared between all the atoms. The remaining two electrons are in bonding ' π_u orbitals' between the carbon atoms ($1b_{3u}$ in the notation of Herzberg 1966). The lowest unoccupied orbital is the anti-bonding ' π_g orbital' between the carbon atoms ($1b_{2g}$).

Assuming that there is not a stable negative ion of ethylene the state of $C_2H_4^-$ obtained by adding an electron in a π_g orbital to C_2H_4 in its ground state should show up as the lowest shape resonance. It is effectively a d-wave resonance like the ground state of N_2^- (§3.2). If, as suggested by the experiment of Boness *et al.*, the state occurs at an energy of 0.2 eV, its width should be extremely small, of the order of 0.001 eV. If, on the other hand, this lower peak at 0.2 eV is not caused by a

resonance and this lowest shape resonance occurs near 1.5 eV, then the expected width would be of the order of 0.1 eV.

There may also be a low-lying electron-excited Feshbach resonance in which the π_u orbital is occupied by only one electron and the higher π_g orbital by two. If the 0.2 eV peak of Boness *et al.* does correspond to the $C_2H_4^-$ ground state then the upper peak could be due to this Feshbach resonance.

The identification of these two resonances would be facilitated by a measurement of the angular distribution of inelastically scattered electrons.

II. Collision processes

7. Resonance formalisms

In part II of this article we shall show how the cross sections of various collision processes can be expressed in terms of the properties of the resonant states, and we shall analyse the results of experimental studies of resonant scattering processes. In this section we shall briefly describe the three resonant scattering formalisms which have been applied to molecular problems.

7.1. The theories of Siegert, and of Kapur and Peierls

In §2 we saw that the time dependence of a resonant state Ψ_n^r is formally the same as that of a stationary state but with a complex energy W_n (equations (2.1)–(2.2)). It follows that Ψ_n^r obeys the time-independent Schrödinger equation

$$H\Psi_n^r = W_n\Psi_n^r \quad (7.1)$$

where H is the Hamiltonian of the system. The bound-state solutions, for which W_n is real and negative, are obtained by demanding that the wave functions should become exponentially small if one or more interparticle separations become large. For a resonant state one must instead demand that for large separations the wave function represents pure outgoing waves due to the decay of the resonance.

For simplicity let us consider s-wave potential scattering. The outgoing-wave boundary condition for the radial wave function $\psi_n(r)/r$ then has the form

$$\frac{d}{dr}\psi_n(r) = i\left(\frac{2mW_n}{\hbar^2}\right)^{1/2}\psi_n(r) \quad (7.2)$$

i.e.

$$\psi_n(r) \simeq \exp\left\{i\left(\frac{2mW_n}{\hbar^2}\right)^{1/2}r\right\}. \quad (7.3)$$

This definition of a resonance as an eigenfunction of the Hamiltonian with this outgoing-wave boundary condition was first introduced by Siegert (1939), and we shall call resonant states defined in this way Siegert states. Since the resonant wave functions are solutions of the wave equation with no incoming waves, their energies W_n give the positions of the poles of the S matrix. This fact can be used as basis for a resonant scattering formalism (Humblert and Rosenfeld 1961).

The Siegert approach has two disadvantages which arise from the occurrence of the resonant energy W_n in the boundary condition (7.2)–(7.3). It makes the

calculation of resonant states more difficult and, more seriously, it means that different Siegert states are not orthogonal.

These difficulties are avoided in the theory of Kapur and Peierls (1938). They define resonant states in the same way as Siegert, except that in the boundary condition (7.2)–(7.3) the resonant energy W_n is replaced by the real energy E of the system. These Kapur–Peierls states form an orthonormal set, in terms of which one can expand the scattering state and hence find the cross sections. The disadvantage of this method is that the properties of the individual resonant states depend somewhat on the energy E and on the value of r at which the boundary condition is imposed.

The study of molecules demands an extension of the resonance theory as applied to atomic and nuclear problems. The method that will be discussed in §§ 8 and 9 contains elements of both the Siegert and Kapur–Peierls theories. As for these two, the essence of the method is that resonant states are defined as eigenstates of the complete Hamiltonian which satisfy outgoing-wave boundary conditions.

7.2. The projection operator formalism of Feshbach

Although resonant states are temporary, their lifetimes are often long on the atomic scale. In these cases the resonant wave function will be very nearly that of a bound state. The Feshbach resonances, discussed in §§ 2.2 and 4, are of this kind. Feshbach (1958, 1962) first stressed the importance of this resonance mechanism and developed the projection operator formalism for handling it.

In this approach, projection operators P and $Q \equiv 1 - P$ are introduced to divide the wave function Ψ into two parts $P\Psi$ and $Q\Psi$. The open-channel component $P\Psi$ has the same asymptotic form as Ψ . It has an outgoing-wave component and so allows an electron to escape to infinity. The closed-channel component $Q\Psi$ vanishes asymptotically for large electron separation. The definition of the projection operators is an asymptotic one and is thus not unique. (This problem is discussed by Burke (1965, §3.2) and by Smith (1966, §5.1) who give examples of some of the definitions of projection operators used in atomic problems. References for molecular problems are given below.) This flexibility in the choice of projection operators is essential in order to ensure that molecular resonant states have the proper dissociation limit. This is necessary for the determination of accurate potential energy curves and is particularly important for a simple treatment of dissociation processes. The correct dissociation limit is obtained by defining $Q\Psi$ to contain an admixture of the target ground state (and, if necessary, other energetically accessible target states). The projection operators P and Q satisfy the relations

$$P + Q = 1, \quad P^2 = P, \quad Q^2 = Q, \quad PQ = 0. \quad (7.4)$$

The Schrödinger equation for the scattering wave function Ψ leads to the following coupled equations for its two parts $P\Psi$ and $Q\Psi$:

$$P(H - E)P\Psi = -PHQ\Psi \quad (7.5)$$

$$Q(H - E)Q\Psi = -QHP\Psi. \quad (7.6)$$

The terms on the right-hand sides of these equations represent the coupling of open and closed channels. If these terms are replaced by zero, the resulting equations are decoupled and describe the scattering in the open channels and the bound-state problem in the closed channels.

If we formally solve (7.6) for $Q\Psi$ and substitute in (7.5) we obtain a single equation for $P\Psi$:

$$P\left\{H - PHQ \frac{1}{Q(H-E)Q} QHP - E\right\} P\Psi = 0. \quad (7.7)$$

The term $P(H-E)P$ is the operator which would have applied if we had retained open-channel components only in Ψ . The effect of the closed-channel components is to introduce into (7.7) the optical potential

$$V_{\text{opt}} = -PHQ \frac{1}{Q(H-E)Q} QHP. \quad (7.8)$$

In order to study the significance of the closed-channel components we introduce the eigenfunctions Ψ_{Qn} of the operator QHQ , defined by the equation

$$QHQ\Psi_{Qn} = E_{Qn}\Psi_{Qn}. \quad (7.9)$$

In terms of these wave functions the optical potential becomes

$$V_{\text{opt}} = -\sum_n PHQ \frac{|\Psi_{Qn}\rangle\langle\Psi_{Qn}|}{E_{Qn} - E} QHP. \quad (7.10)$$

One consequence of this expression is that, provided the experimental energy E is less than all the eigenvalues E_{Qn} , the optical potential is necessarily attractive, and indeed each term in the summation in (7.10) is attractive. From this property of the optical potential one can derive variational bounds for the reactance matrix (Hahn *et al.* 1964).

Let us consider the solution of equation (7.7) for an energy E close to one particular eigenvalue E_{Qn} . We write (7.7) as

$$P(E - H')P\Psi = \frac{PHQ\Psi_{Qn}\rangle\langle\Psi_{Qn}|QHHP|\Psi\rangle}{E - E_{Qn}} \quad (7.11)$$

where

$$H' \equiv H + \sum_{m \neq n} PHQ \frac{|\Psi_{Qm}\rangle\langle\Psi_{Qm}|}{E - E_{Qm}} QHP. \quad (7.12)$$

For E near E_{Qn} the left-hand side of equation (7.11) is then a slowly varying function of energy compared with the right-hand side. If G^+ is the outgoing-wave Green function of equation (7.11) and Ψ_{PE} the solution of the corresponding homogeneous equation, the solution of (7.11) becomes

$$P\Psi = \Psi_{PE} + \frac{G^+ PHQ |\Psi_{Qn}\rangle\langle\Psi_{Qn}| QHP |\Psi_{PE}\rangle}{E - E_{Qn} - \Delta_n} \quad (7.13)$$

where

$$\begin{aligned} \Delta_n &\equiv \langle\Psi_{Qn}|QHHPG^+PHQ|\Psi_{Qn}\rangle \\ &= \int dE' \frac{|\langle\Psi_{Qn}|QHHP|\Psi_{PE'}\rangle|^2}{E - E' + i\epsilon}. \end{aligned} \quad (7.14)$$

Since the asymptotic form of Ψ' is determined by that of $P\Psi'$, equation (7.13) suffices to give the scattering cross section. It can be seen that the cross section will have a pole at the energy $E_{Qn} + \Delta_n$. This gives the connection with the Siegert resonance theory. It shows that an eigenstate of the operator QHQ leads to a resonance at an energy $E_{Qn} + \Delta_n$. The width of this resonance is

$$\Gamma_n = -2\mathcal{I}\Delta_n = 2\pi|\langle\Psi'_{Qn}|QH\Psi'_{PE}\rangle|^2. \quad (7.15)$$

The application of the projection operator formalism to atomic problems has been reviewed by Burke (1965) and Smith (1966). The method has been applied to molecular systems by Chen (1966 b, 1967) and O'Malley (1966, 1967 c). These authors have shown how to obtain cross sections for such processes as dissociative attachment and associative detachment. The application of the method to the calculation of potential curves for resonant states has been demonstrated by Eliezer *et al.* (1967) who have obtained the curves for two states of H_2^- (see § 4.3). They used the bound-state variational method and restricted their wave function to have only closed-channel components. Thus they found the bound states Ψ'_{Qn} which closely approximate the resonant states. They have not calculated the energy shifts or widths associated with the resonances.

7.3. The configuration interaction theory of Fano

This method is very similar to the projection operator approach. Although formally it is not so complete, its simplicity makes it ideal for numerical calculation and for the analysis of experimental results.

The method is based on the independent-particle model for the electrons in atoms or molecules. In this, one approximates the state of the system by a one-configuration wave function. Although an actual state of the system contains a mixture of many different configurations it can often be approximated closely by including only one or two of these configurations.

The mixing of two configurations is of special interest when one belongs to a discrete spectrum and the other to a continuous spectrum. The effect of the mixing is to turn the bound state of the discrete spectrum into an autoionizing or resonant state. The theory of such configuration interaction was first given by Rice (1933) who applied it to predissociation, but the real significance of the approach for resonances in electron scattering and photon absorption was shown by Fano (1935, 1961).

Let Ψ_n^d and $\Psi_{E'}^c$ be approximate wave functions of the system representing different configurations, the state Ψ_n^d belonging to a discrete spectrum and the state $\Psi_{E'}^c$ to a continuous spectrum. Let us consider the mixing of these states, which we take as orthonormal

$$\langle\Psi_{E'}^c|\Psi_n^d\rangle = 0, \quad \langle\Psi_{E'}^c|\Psi_{E''}^c\rangle = \delta(E-E'') \quad (7.16)$$

and satisfying

$$\langle\Psi_{E'}^c|H|\Psi_{E''}^c\rangle = E''\delta(E-E''). \quad (7.17)$$

We define

$$E_n \equiv \langle\Psi_n^d|H|\Psi_n^d\rangle, \quad V_E \equiv \langle\Psi_{E'}^c|H|\Psi_n^d\rangle. \quad (7.18)$$

We assume that the total scattering state Ψ of the system at an energy E can be written

$$\Psi = a\Psi_n^d + \int dE' b_{E'} \Psi_{E'}^c. \quad (7.19)$$

By demanding that

$$\langle \Psi_n^d | H - E | \Psi \rangle = 0, \quad \langle \Psi_{E'}^c | H - E | \Psi \rangle = 0 \quad (7.20)$$

one can determine the coefficients a and $b_{E'}$. This leads to the result

$$\begin{aligned} \Psi = & \Psi_{E'}^c + \frac{V_E^*}{E - E_n - \Delta_n} \Psi_n^d \\ & + \frac{V_E^*}{E - E_n - \Delta_n} \int dE' \frac{V_{E'}}{E - E' + i\epsilon} \Psi_{E'}^c \end{aligned} \quad (7.21)$$

where

$$\Delta_n \equiv \int dE' \frac{|V_{E'}|^2}{E - E' + i\epsilon}. \quad (7.22)$$

The significance of the three terms in (7.21) is clear. The first represents the scattering state in a single-configuration approximation. The second term represents the temporary formation of the discrete state of the other configuration, while the third term gives the scattered wave which results from the formation and decay of that state.

It follows from (7.21) that the cross section will have a pole at the complex energy $E_n + \Delta_n$. The width of the corresponding resonant state is given by

$$\begin{aligned} \Gamma_n = & -2\mathcal{I}\Delta_n = 2\pi|V_E|^2 \\ = & 2\pi|\langle \Psi_n^d | H | \Psi_{E'}^c \rangle|^2. \end{aligned} \quad (7.23)$$

A comparison with equations (7.13)–(7.15) shows that these results of Fano's approach can be derived from the corresponding results of the projection operator formalism by approximating Ψ_{PE} and $Q\Psi$ by $\Psi_{E'}^c$ and Ψ_n^d respectively.

The great success of Fano's theory in electron scattering and photon absorption by atoms arises from its simplicity and its ability to treat the interference between resonant and non-resonant scattering amplitudes, i.e. the third and first terms in (7.21). (The second term in equation (7.21) gives no contribution to the scattering since it decreases exponentially at large distances.)

We have discussed the configuration interaction method for the simple case of one discrete state overlapping with one continuum. Fano (1961) has also given the generalizations to the interaction of one discrete state with many continua or of many discrete states with a single continuum. When one considers autoionizing electronic states of molecules, one nearly always has many discrete states interacting with many continua, because of the vibrational motion of the nuclei. This complication can arise even though there are only two electronic configurations involved. The necessary extension of the theory has been described by Bardsley (1968 a), who showed that for thermal electron-molecule collisions this approach is more suitable than the theory which will be developed in §§ 8 and 9. The Fano approach can also be used in the study of nuclear-excited Feshbach resonances as will be shown in § 12.

8. Definition of molecular resonances

The common feature of the different types of resonances discussed in §2 is that they can decay by electron emission. This implies that resonant states satisfy outgoing-wave boundary conditions corresponding to these decay modes. One can use this property to characterize resonances and this approach due to Siegert (1939) (see also Herzenberg *et al.* 1964, Bardsley *et al.* 1966 a) will now be developed for molecules.

New and important features occur for molecules, as compared with atoms, owing to the extra degrees of freedom associated with the nuclear motion. We shall employ an extension of the Born–Oppenheimer procedure for bound states, i.e. calculate resonances adiabatically with the nuclei fixed in position. Important modifications of this approach are required to allow for the exchange of energy between electronic and nuclear motion which is often very large. This adiabatic approach is of course not possible for nuclear-excited Feshbach resonances (see §§5 and 12).

Let us consider an $(N+1)$ -electron molecular system. We write its Hamiltonian

$$H = H_N(\mathbf{R}) + H_{\text{el}}^{N+1}(\mathbf{r}, q, \mathbf{R}) \quad (8.1)$$

where $H_N(\mathbf{R})$ is the kinetic energy operator of the nuclear motion and H_{el}^{N+1} is the electronic Hamiltonian of the system. The nuclear coordinates are collectively denoted by \mathbf{R} and the coordinates of the target electrons by q , while \mathbf{r} stands for the coordinates of the projectile electron which is incident on the target and is emitted in autoionization. In practice it is necessary and possible to antisymmetrize the theory with respect to projectile and target electrons (see Bardsley *et al.* 1964, 1966 b) but this complicates the details greatly. In order to explain the essential features clearly and simply we shall treat the projectile electron as distinguishable, but shall state the final results in their correct form.

A resonant state $\Psi_n(\mathbf{r}, q, \mathbf{R})$ is defined adiabatically in terms of the electronic Hamiltonian H_{el}^{N+1} by

$$\{H_{\text{el}}^{N+1}(\mathbf{r}, q, \mathbf{R}) - W_n(\mathbf{R})\} \Psi_n(\mathbf{r}, q, \mathbf{R}) = 0. \quad (8.2)$$

The nuclear coordinates \mathbf{R} occur in (8.2) only parametrically, i.e. one calculates with the nuclei fixed at \mathbf{R} . This leads to electronic wave functions Ψ_n and eigenvalues $W_n(\mathbf{R})$ which serve as potential energy terms in the Schrödinger equation for the nuclear motion. This is the adiabatic Born–Oppenheimer procedure which is justified by the large ratio of nuclear to electron mass as a consequence of which the velocities of the nuclei are very slow compared with those of the electrons.

The distinction from the case of bound states arises through the boundary conditions which Ψ_n must satisfy. Let us consider the close-coupling expansion of Ψ_n :

$$\Psi_n(\mathbf{r}, q, \mathbf{R}) = \sum_{\nu} \eta_{\nu}(\Omega, q, \mathbf{R}) \phi_{\nu}^n(r, \mathbf{R}) \quad (8.3)$$

where Ω stands for the polar angles of the projectile electron and η_{ν} represents the target state of the N -electron target molecule, with energy $E_{\nu}^N(\mathbf{R})$, coupled to the angular momentum part of the projectile electron's wave function, i.e. $\phi_{\nu}^n(r, \mathbf{R})$ is the radial wave function of the projectile electron in the channel ν . (We shall use ν

to stand collectively for all quantum numbers of the system or those that are relevant. These quantum numbers specify the nuclear and electronic state of the target molecule and the angular momentum quantum numbers of the projectile.) Kapur and Peierls (1938) then impose the outgoing-wave boundary conditions

$$\left\{ \frac{\partial}{\partial r} \log \phi_\nu^n(r, \mathbf{R}) \right\}_{r=r_0} = F_\nu(\kappa, r_0) \quad (8.4)$$

where

$$F_\nu(\kappa, r) \equiv \frac{\partial}{\partial r} \log \{h_\nu^+(\kappa r)\}; \quad (8.5)$$

h_ν^+ is an outgoing-wave spherical Hankel function and

$$\kappa = \tilde{k}_\nu \equiv \left[\frac{2m}{\hbar^2} \{E - E_\nu^N(\mathbf{R})\} \right]^{1/2}. \quad (8.6)$$

The boundary conditions (8.4) are imposed at a 'joining radius' $r = r_0$ such that for $r > r_0$ the projectile is free, i.e. all the interaction is contained within the internal region $r \leq r_0$. (These are the boundary conditions for a potential of finite range. If the target is a positive ion, or to allow for other long-range effects, one can replace the free-particle wave functions h_ν^+ in (8.4)–(8.5) by Coulomb or distorted waves.) Equation (8.6) defines the energy $\hbar^2 \tilde{k}_\nu^2 / 2m$ for the electron to autoionize into channel ν , the total energy of the system being E and the nuclei being held fixed at \mathbf{R} all the time.

Equations (8.4)–(8.6) are the boundary conditions one would have for atoms. They will not do for molecules in general, because of the considerable exchange of energy between the electronic and nuclear motion. It may happen that *all* the available energy of the resonance is transferred to the nuclear motion so that no energy is available for electron emission. This is the basic mechanism of dissociative attachment. The boundary conditions for electron emission then depend on the nuclear motion, i.e. on the complete solution, leading to a very complicated self-consistency condition. Fortunately, in the case of a single electronic resonance it can be shown (Bardsley *et al.* 1964, 1966 b) that the correct boundary conditions reduce to equations (8.4)–(8.5) with

$$\kappa = k_{n\nu} \equiv \left[\frac{2m}{\hbar^2} \{W_n(\mathbf{R}) - E_\nu^N(\mathbf{R})\} \right]^{1/2}. \quad (8.7)$$

This definition of the resonant state is independent of the nuclear motion and of the energy of the system; it is precisely that of a Siegert state. It can be shown that for fixed \mathbf{R} , $W_n(\mathbf{R})$ is a pole of the scattering matrix in the complex energy plane. This definition of a Siegert state is independent of the choice of joining radius r_0 provided it is beyond the range of the interactions of the projectile with the target. (In the Kapur–Peierls definition such a spurious r_0 dependence does occur.) In the case of long-range interactions one must either truncate and neglect these beyond a certain distance or use distorted waves in the boundary conditions (8.4)–(8.5), just as in the Kapur–Peierls theory.

Because of the complex boundary conditions, the energy eigenvalue $W_n(\mathbf{R})$ is, in general, complex:

$$W_n(\mathbf{R}) \equiv E_n(\mathbf{R}) - \frac{1}{2}i\Gamma_n(\mathbf{R}) \quad (8.8)$$

where $\Gamma_n(\mathbf{R})$ is the width of the decaying state and $\hbar/\Gamma_n(\mathbf{R})$ its lifetime. Siegert's definition of a resonance is analogous to that of a bound state into which it goes over for W_n real and negative.

It follows from (8.7) that the wave-vectors $k_{n\nu}$ are complex. Consequently the Siegert-state wave functions diverge exponentially at large distances. (Physically this corresponds to the fact that, in a time-dependent picture, the wave function at large distances must have leaked out from the decaying resonant ion at very much earlier times when its wave function had a much larger amplitude.) Because of this exponential divergence it is necessary to restrict integrals involving Siegert-state wave functions to finite domains of integration only.

One can calculate Siegert states from a modified form of the Rayleigh-Ritz variational principle which incorporates surface terms which lead to the Siegert outgoing-wave boundary conditions (8.4)–(8.5). Herzenberg and Mandl (1963) have given such a variational principle for resonances defined with Kapur-Peierls boundary conditions; this can be extended, by an iteration procedure, to cope with Siegert boundary conditions. This method has been applied successfully to the 3 eV and 10 eV resonances of H_2^- (Bardsley *et al.* 1966 a). The advantage of this method is that it gives both the real part and the imaginary part (i.e. the width) of the resonance energy W_n variationally.

Alternative variational methods for calculating resonant states are discussed by Taylor *et al.* (1966). They depend on suitably restricting the trial functions. For Feshbach resonances this is easily achieved by decoupling open and closed channels using projection operators or, equivalently, restricting the trial wave functions to contain closed-channel components only. Taylor *et al.* (1966) have refined these methods to apply also to shape resonances, and have successfully used these methods to calculate the 3 eV, 10 eV and 12 eV resonances of H_2^- (Eliezer *et al.* 1967). So far these methods have only given $E_n(\mathbf{R})$, the position of the resonance, and not its width $\Gamma_n(\mathbf{R})$.

From equation (8.2) and its complex conjugate an expression can be derived for the width $\Gamma_n(\mathbf{R})$. For the completely antisymmetrized theory this reads (Bardsley *et al.* 1966 b)

$$\Gamma_n(\mathbf{R}) = \frac{(\hbar^2 r_0^2/m)(N+1) \sum_\nu |\phi_\nu^n(r_0, \mathbf{R})|^2 \mathcal{S}F_\nu(k_{n\nu}, r_0)}{\int_{\Omega(r_0)} \prod_{i=1}^{N+1} d\mathbf{r}_i |\Psi_n|^2} \quad (8.9)$$

where $\Omega(r_0)$ is the internal region, i.e. all $r_i \leq r_0$, as discussed earlier in this section.

Equation (8.9) is typical for a total width. It consists of contributions from the different channels ν , each contribution depending on a reduced width (proportional to $|\phi_\nu^n(r_0, \mathbf{R})|^2$) and a barrier penetration factor (proportional to $\mathcal{S}F_\nu(k_{n\nu}, r_0)$). If we approximate $W_n(\mathbf{R})$ in (8.7) by $E_n(\mathbf{R})$, which is justified for a narrow resonance, then it follows from (8.9) that only open channels ($E_n(\mathbf{R}) > E_\nu^N(\mathbf{R})$) contribute to the width. It is possible to re-express equation (8.9) in terms of a matrix element for the interaction of the projectile with the target molecule (Herzenberg *et al.* 1964, Kwok and Mandl 1965).

9. The nuclear wave equation

9.1. Derivation of the nuclear wave equation

We next derive the wave equation for the nuclear motion. As in the usual Born–Oppenheimer theory, this will contain the eigenvalue $W_n(\mathbf{R})$ of the electronic problem (8.2) as potential. This potential is now complex corresponding to the decaying nature of the electronic state Ψ_n . As a second new feature the nuclear wave equation may contain a ‘feeding term’ corresponding to the formation of the resonant state through electron capture by the target molecule.

The wave function of the complete system satisfies

$$(H - E)\Psi(\mathbf{r}, q, \mathbf{R}) = 0. \quad (9.1)$$

We write

$$H_{\text{el}}^{N+1}(\mathbf{r}, q, \mathbf{R}) = H_{\text{el}}^N(q, \mathbf{R}) + K_0 + V(\mathbf{r}, q, \mathbf{R}) \quad (9.2)$$

where H_{el}^N is the electronic target Hamiltonian, K_0 the kinetic energy operator of the projectile electron and V its interaction with the target. We put

$$\Psi(\mathbf{r}, q, \mathbf{R}) = \zeta_\mu(\mathbf{R})\Phi_\mu(\mathbf{r}, q, \mathbf{R}) + \Psi_{\text{sc}}(\mathbf{r}, q, \mathbf{R}) \quad (9.3)$$

where Ψ_{sc} is the scattered wave and $\zeta_\mu\Phi_\mu$ the wave function of the initial target state plus the non-interacting incident projectile electron. Φ_μ is the adiabatic electronic wave function

$$\Phi_\mu(\mathbf{r}, q, \mathbf{R}) = \chi_\mu(q, \mathbf{R}) \exp(i\mathbf{k}_\mu \cdot \mathbf{r}) \quad (9.4)$$

with χ_μ , the initial target state, satisfying

$$\{H_{\text{el}}^N(q, \mathbf{R}) - E_\mu^N(\mathbf{R})\}\chi_\mu(q, \mathbf{R}) = 0; \quad (9.5)$$

ζ_μ is the initial nuclear wave function which satisfies

$$\{H_N + E_\mu^N(\mathbf{R}) - \epsilon_\mu\}\zeta_\mu(\mathbf{R}) = 0. \quad (9.6)$$

The total energy E of the system, the energy ϵ_μ of the initial target state and the kinetic energy of the incident projectile are related by

$$E = \epsilon_\mu + \frac{\hbar^2 k_\mu^2}{2m}. \quad (9.7)$$

μ labels the quantum numbers of the initial state $\zeta_\mu\Phi_\mu$ which will usually be the ground state of the target molecule and for simplicity we shall refer to it as such.

Using the fact that the electronic wave function $\chi_\mu(q, \mathbf{R})$ is a slowly varying function of \mathbf{R} compared with the nuclear wave function $\zeta_\mu(\mathbf{R})$ and equations (8.1) and (9.2) to (9.7), we can rewrite equation (9.1) in the form

$$\begin{aligned} \{H_N + H_{\text{el}}^{N+1}(\mathbf{r}, q, \mathbf{R}) - E\}\Psi_{\text{sc}}(\mathbf{r}, q, \mathbf{R}) \\ = -V(\mathbf{r}, q, \mathbf{R})\zeta_\mu(\mathbf{R})\Phi_\mu(\mathbf{r}, q, \mathbf{R}). \end{aligned} \quad (9.8)$$

We shall restrict ourselves to resonant processes which at a given energy E are due to a *single* electronic resonance state Ψ_n . The scattered wave is then due solely to the decay of this single electronic resonance. We shall assume that the scattered

wave can be written as the product of the adiabatic electronic wave function Ψ_n and a nuclear wave function $\tilde{\xi}_n(\mathbf{R})$:

$$\Psi_{sc}(\mathbf{r}, q, \mathbf{R}) = \tilde{\xi}_n(\mathbf{R}) \Psi_n(\mathbf{r}, q, \mathbf{R}). \quad (9.9)$$

Equation (9.8) then becomes, on account of (8.2) and again using the adiabatic approximation to replace $H_N(\tilde{\xi}_n \Psi_n)$ by $\Psi_n(H_N \tilde{\xi}_n)$,

$$\begin{aligned} \{H_N + W_n(\mathbf{R}) - E\} \tilde{\xi}_n(\mathbf{R}) &= \tilde{J}_n(\mathbf{R}) \\ &\equiv -\zeta_\mu(\mathbf{R}) \int_{\Omega(r_0)} d\mathbf{r} dq \Psi_n^\dagger(\mathbf{r}, q, \mathbf{R}) V(\mathbf{r}, q, \mathbf{R}) \Phi_\mu(\mathbf{r}, q, \mathbf{R}). \end{aligned} \quad (9.10)$$

Here Ψ_n is normalized by

$$\int_{\Omega(r_0)} d\mathbf{r} dq \Psi_n^\dagger \Psi_n = 1 \quad (9.11)$$

$\Omega(r_0)$ being the internal region defined in § 8. Ψ_n^\dagger is defined by replacing, in equation (8.3), Ψ_n by Ψ_n^\dagger and the η_ν by their complex conjugates η_ν^* .

The nuclear wave equation (9.10) is our basic result. It is fundamental for molecular collision processes involving resonances. It displays the two characteristic features mentioned above: it has a complex potential corresponding to the decaying nature of the resonance, and it has the feeding term $\tilde{J}_n(\mathbf{R})$, proportional to the amplitudes of the incident electron beam and of the initial molecular state, which is responsible for the generation of the resonance through electron capture by the target molecule. For processes such as associative detachment, where there is no incident electron current, the nuclear wave equation (9.10) still holds, with $\tilde{J}_n(\mathbf{R})$ replaced by zero. An alternative form of the feeding term in (9.10) can be derived from the equations satisfied by Φ_μ and Ψ_n^\dagger . (It is here that the use of Ψ_n^\dagger rather than Ψ_n^* is essential.) This form, in terms of surface amplitudes $\phi_\mu^n(r_0, \mathbf{R})$ in the *incident* channel, is given by Bardsley *et al.* (1964, 1966 b) who also obtain a more general form for the nuclear wave equation, valid when more than one electronic resonance is important.

In order to solve the nuclear wave equation (9.10), we shall assume that the lifetime of the resonant molecular ion is short compared with its rotational periods. In practice this is usually the case. One may then neglect the kinetic energy of the rotational motion in (9.10) compared with the vibrational and electronic energies. This amounts to keeping the molecular axis fixed during the lifetime of the complex and treating the rotations classically by averaging over all initial orientations of the molecular axis. This is equivalent to averaging over initial and summing over final angular momentum states of the system. Restricting ourselves to diatomic molecules, for which most theoretical work has been done, we may then replace \mathbf{R} by R , the internuclear distance. We now put

$$\tilde{\xi}_n(\mathbf{R}) \equiv \frac{\xi_n(R, \mathbf{k}_\mu)}{R}, \quad \tilde{J}_n(\mathbf{R}) \equiv \frac{J_n(R, \mathbf{k}_\mu)}{R}$$

where the argument \mathbf{k}_μ has been added to show the dependence of ξ_n and J_n on the relative orientation of the incident electron beam and the molecular axis, now held

fixed. The nuclear wave equation (9.10) then becomes

$$\left\{ -\frac{\hbar^2}{2M} \frac{d^2}{dR^2} + W_n(R) - E \right\} \xi_n(R, \mathbf{k}_\mu) = J_n(R, \mathbf{k}_\mu) \quad (9.12)$$

where M is the reduced mass of the nuclei.

The way in which equation (9.12) describes dissociative attachment can be understood from figure 15. The nuclei are initially vibrating in the potential $E_\mu^N(R)$ with wave function $\zeta_\mu(R)$. As a result of electron capture at internuclear distance R_E , the nuclei start to move in the modified potential $W_n(R)$ with the wave

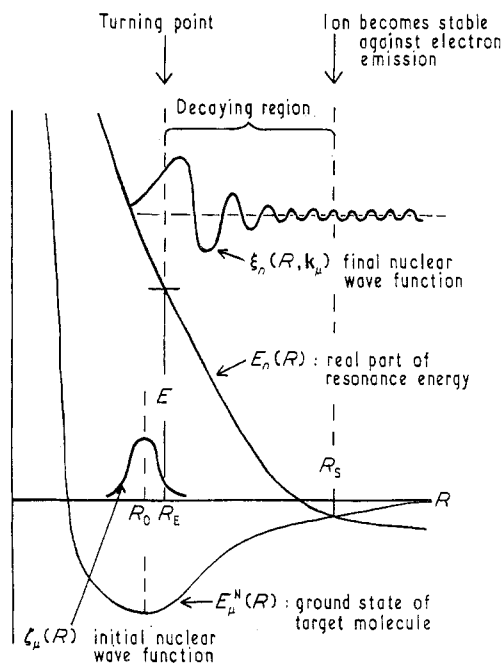


Figure 15. Potential energy curves and nuclear wave functions in dissociative attachment. The final wave function is schematic only. (From Bardsley *et al.* 1966 b.)

function $\xi_n(R, \mathbf{k}_\mu)$ which has a decaying amplitude for $R_E \leq R \leq R_S$ due to the possibility of the autoionization, leaving the nuclei in an excited state or the ground state of the potential $E_\mu^N(R)$. Depending on the lifetime of the resonance, the nuclei may separate to a distance R_S without autoionization having occurred. This corresponds to dissociative attachment. For R greater than the stabilization distance R_S electron emission is no longer energetically possible, the width Γ_n vanishes and ξ_n oscillates with a constant amplitude which determines the dissociative attachment cross section.

The nuclear wave equation (9.12) describes the nuclear motion in terms of a complex *local* potential. Most previous applications have been of this form. It has been pointed out by Bardsley (1968 a) that this equation is only applicable if the energy of the scattered electron is large compared with the vibrational spacings of the negative ion complex. For processes at thermal energies, such as dissociative

recombination, this is not the case and a description in terms of a non-local potential is required (Bardsley 1968 a, O'Malley 1967 b).

9.2. Solution of the nuclear wave equation

In order to solve the nuclear wave equation (9.12) we introduce the Green function $G_n(R, R')$ which satisfies

$$\left\{ -\frac{\hbar^2}{2M} \frac{d^2}{dR^2} + W_n(R) - E \right\} G_n(R, R') = \delta(R - R'). \tag{9.13}$$

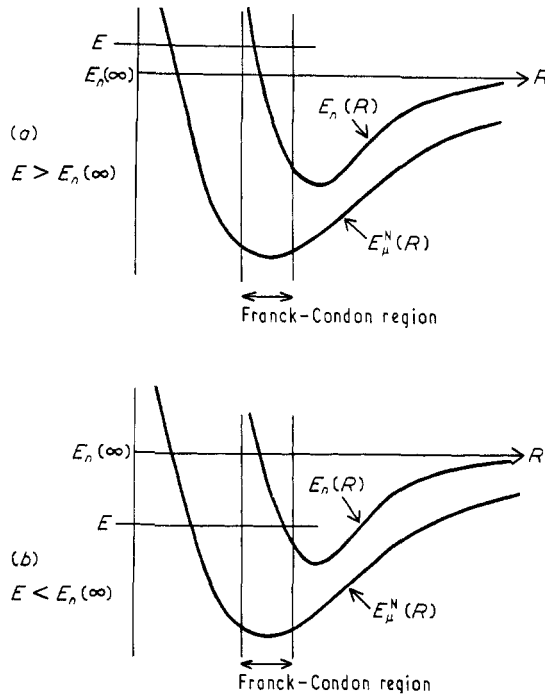


Figure 16. Potential energy curves $E_\mu^N(R)$ and $E_n(R)$ of the target ground state and of the resonant state respectively. (a) $E > E_n(\infty)$. (b) $E < E_n(\infty)$.

The solution of (9.12) is then given by

$$\xi_n(R, \mathbf{k}_\mu) = \int_0^\infty dR' G_n(R, R') J_n(R', \mathbf{k}_\mu). \tag{9.14}$$

Physically two different situations arise according as to whether

$$E \geq \mathcal{R}W_n(R = \infty) = E_n(R = \infty)$$

i.e. according as to whether dissociation can or cannot occur at the energy E of the system. The potential energy curves for the two cases are illustrated in figure 16.

Correspondingly, the Green function satisfies different boundary conditions at infinity: outgoing-wave boundary conditions for $E > E_n(\infty)$ and bound-state boundary conditions for $E < E_n(\infty)$. The boundary condition at the origin is $G_n(0, R') = 0$ in both cases.

Let $u_I^n(R)$ and $u_{II}^n(R)$ be solutions of (9.13) with the right-hand side replaced by zero and satisfying the same boundary conditions at $R = 0$ and $R = \infty$ respectively as $G_n(R, R')$. The Green function is then given by

$$G_n(R, R') = \frac{u_{II}^n(R_{>}) u_I^n(R_{<})}{u_I^n(d/dR) u_{II}^n - u_{II}^n(d/dR) u_I^n} \quad (9.15)$$

where the denominator is a constant independent of R , and $R_{>}$ and $R_{<}$ are respectively the greater and the lesser of R and R' .

The expression (9.15) for the Green function is generally valid. However, if $E < E_n(\infty)$ and $E_n(R)$ possesses a minimum, as illustrated in figure 16(b), it may be convenient to use a different form. For in this case the vibrational states of the nuclei, moving in the resonance potential $W_n(R)$, will give characteristic structure to the elastic and inelastic scattering cross sections. Let $u_n(E', R)$ be the complete set of real eigenfunctions, with eigenvalues E' , satisfying

$$\left\{ -\frac{\hbar^2}{2M} \frac{d^2}{dR^2} + E_n(R) - E' \right\} u_n(E', R) = 0 \quad (9.16)$$

and the boundary conditions $u_n(E', 0) = 0$; $u_n(E', R)$ is a bound state or standing wave for $E' \leq E_n(\infty)$, respectively, at $R = \infty$. From (9.13) one finds directly that

$$G_n(R, R') = \sum_{E'} \frac{u_n(E', R) u_n(E', R')}{E' - E - \frac{1}{2}i\Gamma_n(R)} \quad (9.17)$$

where $\sum_{E'}$ stands for summation over the discrete spectrum ($E' < E_n(\infty)$) and integration over the continuous spectrum ($E' > E_n(\infty)$). Equation (9.17) is exact. In practice it is of use if it can be approximated by retaining only a few terms of the discrete spectrum and dropping the continuum contribution.

10. Dissociative attachment

10.1. The cross section for dissociative attachment

We now consider the process of dissociative attachment which may occur whenever one of the atoms of the target molecule possesses a stable negative ion. In this case there will exist resonant states which have the correct asymptotic form to describe dissociative attachment. In particular, for nuclear separations R greater than the stabilization distance R_s the complex becomes stable against electron emission. We shall assume that at a given energy only one electronic resonance state is of importance for this process. The mechanism of this process was described in §9 (see figure 15). It depends exclusively on the resonance and ignores the non-adiabatic terms in the Hamiltonian which, in general, make only a small contribution to the dissociative attachment process. The resonance process has been considered by Bardsley *et al.* (1964, 1966 b), Chen (1963, 1966 b) and O'Malley (1966). The last two authors use the projection operator formalism and also consider direct and non-adiabatic transitions.

Equation (9.14) for $\xi_n(R, \mathbf{k}_\mu)$ gives the outgoing current for $R \rightarrow \infty$. The total dissociative attachment cross section σ_{DA} is then given by

$$\sigma_{\text{DA}} = \frac{m}{\hbar k_\mu} \frac{\hbar K}{M} \left\{ \frac{2S_n + 1}{2(2S_\mu + 1)} \right\} \lim_{R \rightarrow \infty} \int \frac{d\mathbf{k}_\mu}{4\pi} |\xi_n(R, \mathbf{k}_\mu)|^2 \quad (10.1)$$

where we have included the correct statistical spin factors. (S_n and S_μ are the spins of the resonant and initial target states.) $\hbar K/M$ and $\hbar k_\mu/m$ are the velocities of the emitted negative ion and of the incident electron, and the operation $\int d\mathbf{k}_\mu/4\pi$ averages over all orientations of the molecular axis relative to the unit vector \mathbf{k}_μ which defines the direction of incidence of the electron beam.

In order to calculate σ_{DA} from (10.1) we require the solution of the nuclear wave equation. This is given by equations (9.14), (9.15) and expression (9.10), or some alternative form, for the feeding term $J_n(R, \mathbf{k}_\mu)$. In practice one will have to solve this equation numerically. But the physical features are well displayed in an approximate analytic solution which uses the WKB approximation and assumes that the resonance is narrow. The cross section (10.1) then becomes (Bardsley *et al.* 1966 b)

$$\sigma_{\text{DA}} = \sigma_{\text{cap}} \exp \left\{ - \int_{R_E}^{R_s} \frac{\Gamma_n(R)}{\hbar} \frac{dR}{v(R)} \right\} \quad (10.2)$$

with

$$\begin{aligned} \sigma_{\text{cap}} &= \frac{4\pi^{3/2}}{k_\mu^2} \frac{2S_n + 1}{2(2S_\mu + 1)} \frac{\Gamma_c(R_E)}{2W_1 a} \\ &\times \exp \left[- \frac{\{E - E_n(R_0)\}^2 - \Gamma_n^2(R_0)/4}{W_1^2 a^2} \right] \end{aligned} \quad (10.3)$$

and

$$\Gamma_c(R_E) \equiv (N+1) \frac{\hbar^2 k_\mu}{m} \sum \left| \frac{\phi_\mu^n(r_0, R_E)}{k_\mu \hbar_\mu^+(k_\mu r_0)} \right|^2 \quad (10.4)$$

The summations in (10.4) are with respect to the orbital angular momentum quantum number, and its z component, of the incident electron. The distances R_s , R_0 and R_E , shown in figure 15, are the stabilization distance, the equilibrium separation of the nuclei in the initial state χ_μ of the target molecule and the classical turning point of the resonance potential defined by $E = E_n(R_E)$. a is the vibrational amplitude of the initial nuclear wave function ζ_μ , and

$$-W_1 = \left. \left(\frac{\partial E_n(R)}{\partial R} \right) \right|_{R=R_E} \quad (10.5)$$

denotes the slope of the resonance potential at the turning point.† $v(R)$, in (10.2), is the relative velocity of the nuclei at separation R .

The two factors in equation (10.2) have a simple interpretation. σ_{cap} is the capture cross section for formation of the resonant negative ion (this will be shown below) and the exponential factor, called the survival factor, represents the probability that the negative ion survives from its formation at nuclear separation R_E till

† The notation has been slightly changed compared with Bardsley *et al.* (1966 b). The quantities now denoted by a , R_0 and R_E , were previously called $\alpha^{-1/2}$, \bar{R}_0 and R_0 respectively. It should also be noted that the definition of a is slightly different from that used by Herzenberg and Mandl (1962).

stabilization occurs at separation R_S . This interpretation follows from the fact that $dR/v(R)$ is the time taken by the nuclei to separate from R to $R + dR$ while $\Gamma_n(R)/\hbar$ is the decay rate at this separation. The representation of σ_{DA} as a product of two factors with the above interpretation is not restricted to this approximate analytic solution but is always possible if the rotational energy is neglected in the nuclear wave equation. It is therefore convenient to write σ_{DA} approximately in the form

$$\sigma_{DA} = \sigma_{\text{cap}} \exp\left(\frac{-\bar{\Gamma}_n \tau}{\hbar}\right) \quad (10.6)$$

where σ_{cap} represents a capture cross section, τ is the time the nuclei take to slide apart from R_E to R_S and $\bar{\Gamma}_n$ is a corresponding mean total autoionization width.

Equation (10.4) for $\Gamma_c(R_E)$ has the form of a partial width for capture by (or decay into) the initial molecular state. The capture width Γ_c and the total autoionization width Γ_n are the same only if the incident channel is the only open channel. But in general they may be of quite different magnitudes. This can lead to interesting effects of a small dissociative attachment cross section (small entrance width Γ_c) but a wide resonance none the less (decay to excited states). This happens for the 10 eV resonance of H_2^- .

Since $2W_1 a$ represents the variation of $E_n(R)$ over the range of the nuclear ground-state oscillations, the term $\Gamma_c(R_E)/2W_1 a$ in (10.3) is the fraction of time during which electron capture by the target molecule into the resonant state can occur. Hence we interpret (10.3) as the capture cross section for formation of the negative ion. The main energy dependence of σ_{DA} comes from the exponential factor in σ_{cap} , which leads to a Gaussian peak centred at $E = E_n(R_0)$ and of width (at half-height) $2W_1 a(\log 2)^{1/2}$. This width should not be confused with the width of the electronic resonance.

The dependence of σ_{DA} on the reduced nuclear mass M leads to very interesting isotope effects. The most important effect arises from the survival factor. Since the forces which different isotopes experience are the same, the nuclear velocities $v(R)$ are proportional to $M^{-1/2}$. Hence the separation time τ , and therefore the exponent of the survival factor (10.6), will be proportional to $M^{1/2}$. This can lead to very large isotope effects, the heavier isotope having the smaller cross section. This isotope effect of the survival factor was first predicted by Demkov (1965). σ_{cap} also leads to isotope effects since the vibrational amplitude a which occurs in two places in (10.3) is proportional to $M^{-1/4}$. The occurrence of a in the Gaussian in (10.3) has two effects. It leads to an isotope dependence for the width of the cross section peak and for the magnitude of the cross section which is of the same form, $\exp(\text{const.} \sqrt{M})$, as that of the survival factor. At the peak energy the constant is positive, leading to an enhanced cross section for the heavier isotope. For the survival factor the exponent is always negative. Because of this identical M dependence, it may be difficult to apportion the exponential isotope dependence between these two effects. In general the isotope effects resulting from the Gaussian factor are small but these effects may become important in the case of 'vertical onset', i.e. if the threshold energy for dissociative attachment is much larger than the peak energy $E_n(R_0)$. This is probably the explanation of the observed isotope effect in the 14 eV peak for H_2 , HD and D_2 , and it is probably also relevant for the 3.75 eV peak in H_2 (O'Malley 1966) which will be discussed in §10.2. Finally, the vibrational

amplitude a in the denominator of (10.3) makes σ_{cap} proportional to $M^{1/4}$ which is again a weak effect.

The effect of the centrifugal term in the nuclear wave equation on dissociative attachment has been studied by Chen and Peacher (1967). It would appear not to produce any significant effects except at very low energies.

The formalism for dissociative attachment which has here been described applies, with appropriate changes, to the very similar process of dissociative recombination (Bates 1950, Bardsley 1968 b). The dissociative recombination coefficient α is defined as the product of the dissociative recombination cross section σ_{DR} with the electron velocity v_e , averaged over the Maxwellian velocity distribution of the electrons at the electron temperature T , i.e. in terms of the electron energy $E = \frac{1}{2}mv_e^2$

$$\begin{aligned}\alpha &= \langle \sigma_{\text{DR}}(E) v_e \rangle \\ &= \left\{ \frac{2^3}{m\pi(kT)^3} \right\}^{1/2} \int \sigma_{\text{DR}}(E) \exp\left(\frac{-E}{kT}\right) E dE.\end{aligned}\quad (10.7)$$

In the remainder of this section we shall give examples of dissociative attachment which illustrate the various features which we have discussed.

10.2. Dissociative attachment in H_2 at low energies

In §3.1 we discussed the H_2^- resonance at about 3 eV which has the structure $(1s\sigma_g)^2(2p\sigma_u)^2\Sigma_u^+$. The curves for the potential energy and width were shown in figures 3, 11 and 4. In the Franck–Condon region of the H_2 ground state this resonance can autoionize leading to vibrational excitation (§11.3). But dissociative attachment may also occur provided it is allowed energetically. Since the threshold for dissociative attachment is 3.75 eV, it follows from figures 3 or 11 that the electron capture must take place to the left of the Franck–Condon region leading to a vertical onset for the dissociative attachment cross section σ_{DA} . Precisely this shape has been observed by Schulz and Asundi (1965, 1967). Their results for H_2 are shown in figure 17. Schulz and Asundi measured σ_{DA} for H_2 , HD (in this case the D^- current was measured) and D_2 and obtained peak values of 1.6×10^{-21} , 1×10^{-22} and 8×10^{-24} cm² respectively, all peaks occurring at 3.75 eV. The smallness of these cross sections is a consequence of the short lifetime of this broad shape resonance. Their relative magnitudes are in excellent agreement with the isotope dependence: $\sigma_{\text{DA}} \propto \exp(\text{const.}\sqrt{M})$, discussed in §10.1, with a negative constant, i.e. the survival factor outweighs the Gaussian exponential. Schulz and Asundi attribute the whole isotope effect to the survival factor but we do not believe that a definite conclusion is possible on the basis of existing experimental and theoretical results.

10.3. Dissociative attachment in H_2 near 10 eV

The cross section for dissociative attachment in H_2 was first measured by Khvostenko and Dukel'skii (1957) and Schulz (1959). More recently, measurements in H_2 , HD and D_2 have been reported by Rapp *et al.* (1965) whose results are shown as the broken curves in figure 18, the continuous curves being the

theoretical results of Bardsley *et al.* (1966 b). (These were obtained from a numerical integration of the nuclear wave equation and not from the approximate analytic treatment on which we shall base our discussion.) These results were obtained

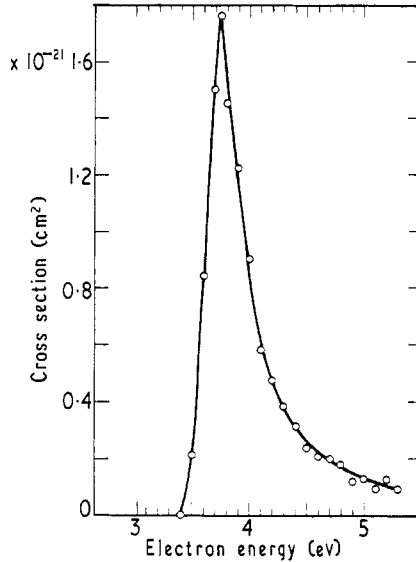


Figure 17. Cross section for H^- formation from H_2 at low energies. (Width of electron energy distribution at half-maximum about 0.1 eV.) (From Schulz and Asundi 1967.)

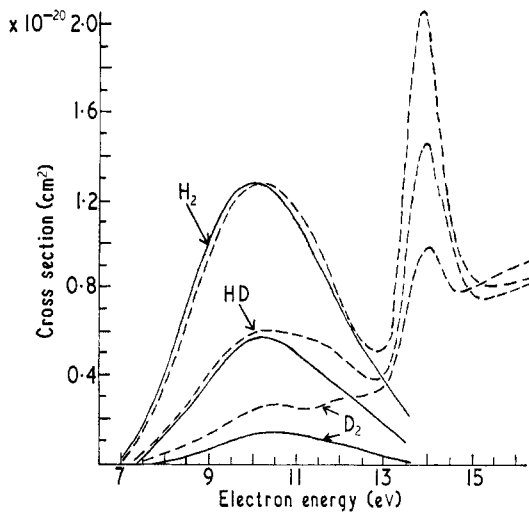


Figure 18. Cross section for dissociative capture in H_2 , HD and D_2 . Full curves, calculations by Bardsley *et al.* (1966 b); broken curves, experimental results by Rapp *et al.* (1965). (From Bardsley *et al.* 1966 b.)

assuming that this process proceeds via the 10 eV $^2\Sigma_g^+$ resonance of H_2^- (Bardsley *et al.* 1966 a), discussed in §6.1. The potential energy curve and width of this resonance are shown in figures 9 and 10, while figure 11 shows a more recent

potential energy curve of Eliezer *et al.* (1967). From these potential energy curves one can conclude that the isotope effect observed by Rapp *et al.* is exclusively due to the survival factor in equation (10.6) giving a mean autoionization width $\bar{\Gamma}_n \simeq 0.8$ ev. The observed magnitude of the peak cross section in H_2 then determines the capture width, equation (10.4), as $\Gamma_c(R_0) \simeq 0.004$ ev. (This width becomes much larger for R greater than about 3 A.U.; see § 6.1.) These results are consistent with the $(1s\sigma_g)(2p\sigma_u)^2 {}^2\Sigma_g^+$ structure of this resonance and the fact that, according to Bardsley *et al.* (1966 a), its potential energy curve lies above the repulsive $(1s\sigma_g)(2p\sigma_u) {}^3\Sigma_u^+$ state of H_2 for not too large nuclear separations R . Hence decay to this state of H_2 can easily occur making a large contribution to $\bar{\Gamma}_n$. On the other hand, in the Franck–Condon region the resonance contains only a small component of the H_2 ground state, resulting in a small capture width $\Gamma_c(R_0)$.

The calculations of Eliezer *et al.* make the potential energy curve of the ${}^2\Sigma_g^+$ resonance cross the ${}^3\Sigma_u^+$ state of H_2 in the Franck–Condon region as shown in figure 11. Decay to the ${}^3\Sigma_u^+$ H_2 state can now occur only to the left of this cross-over leading to a reduction in $\bar{\Gamma}_n$. This is consistent with the results of Bardsley *et al.* (1966 b), who had to scale the calculated total decay width by a factor 0.54 to obtain agreement with experiment. Eliezer *et al.* attribute the dip which is observed in the dissociative attachment cross sections at 11.2 ev to a threshold effect resulting from this new decay channel ${}^3\Sigma_u^+$ opening up at this energy.

Recently Dowell and Sharp (1968) have reported structure in the dissociative attachment cross section of H_2 in the energy range 11.2–12.5 ev. Eliezer *et al.* conjecture that this is due to an interference effect between the 10 ev H_2^- resonance and the two higher-lying ${}^2\Sigma_g^+$ resonances of H_2^- discussed in § 4.3 (see figures 7 and 11) which at these energies lie close together. They furthermore attribute the peak observed at 14 ev in dissociative attachment (see figure 18) to these resonances.

10.4. Dissociative attachment in hot O_2

A strong temperature dependence, in the range 300 °K to 2000 °K, for the position, width and magnitude of the cross-section peak for dissociative attachment in O_2 has been observed (Fite and Brackmann 1963, Fite *et al.* 1965). The circles in figure 19 show these experimental results for 300 °K and 2100 °K while the continuous curves are the theoretical results of O'Malley (1967 a), to be discussed below (see this paper by O'Malley for a discussion of the normalization of these curves).

Demkov (1965) qualitatively interpreted this temperature dependence as due to the contributions from the different vibrational states of O_2 . Detailed calculations by O'Malley (1967 a) of the dissociative attachment cross section for vibrationally and rotationally excited O_2 confirmed this. The surprisingly large effect is due to the sensitivity of the survival factor in equation (10.6). This is illustrated in figure 20 which shows schematically the potential energy curves of the O_2 ground state and of the O_2^- resonance. Let us consider dissociative attachment from the vibrational ground state $v_0 = 0$ and the excited vibrational level $v > 0$. The effective threshold energies for dissociative attachment from these levels correspond to the ordinates AA' and BB'. This explains the shift to lower energies and the broadening of the cross-section peaks for the higher vibrational states. Furthermore, the minimum

separation time τ (BS) for the nuclei to slide apart from the initial separation (at B) to the stabilization distance R_S (at S) for the excited state $v > 0$ is shorter than the corresponding time τ (AS) for the ground state $v_0 = 0$. Hence the survival factor will be smaller for dissociation from the ground state $v_0 = 0$ than from an excited state $v > 0$ which explains the larger cross sections at higher temperatures. O'Malley

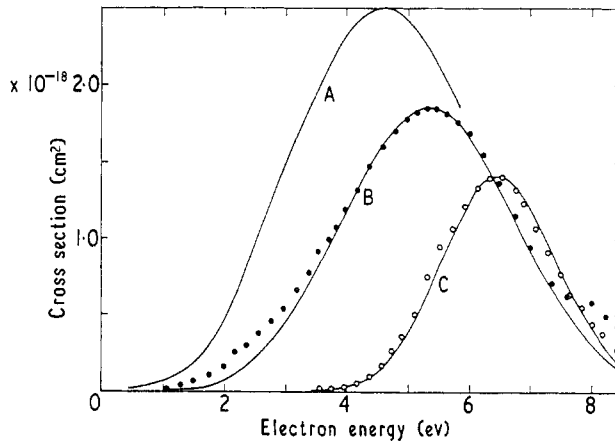


Figure 19. Dissociative attachment cross section in O_2 at 3000 °K (curve A), 2100 °K (curve B) and 300 °K (curve C). The circles are the experimental points of Fite *et al.* (1963, 1965). The full curves are the theoretical results of O'Malley (1967 a).

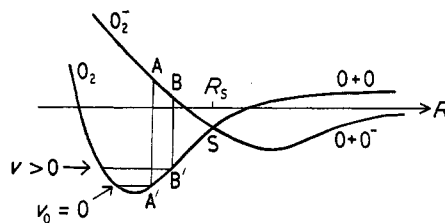


Figure 20. Schematic diagram of the potential energy curves of the O_2 ground state and of the O_2^- resonance.

has calculated the dissociative attachment cross section in this way allowing for the Boltzmann distributions, at different temperatures, over the vibrational and rotational levels of O_2 , and for the energy spectrum of the electron beam used by Fite *et al.* The agreement shown in figure 19 between theory and experiment shows that this interpretation of the temperature dependence is correct. As expected, O'Malley's calculations show that the main effect stems from the excitation of the first few vibrational levels while the rotations and the spread in electron energies are not very important.

10.5. Dissociative attachment in methane

Sharp and Dowell (1967) have measured the H^- and D^- production in dissociative attachment in CH_4 and CD_4 in the energy range 8 to 13 eV and observed

the isotope effect

$$\sigma_{\text{DA}}(\text{CD}_4) \simeq 1.25 \sigma_{\text{DA}}(\text{CH}_4).$$

This is the only case known to us where the cross section of the heavier isotope is the larger one. Although the theory developed in § 10.1 was for diatomic molecules, the form (10.6) for σ_{DA} as the product of a capture cross section σ_{cap} and a survival factor will clearly hold for any two-body break-up. Assuming that the observed process is of this kind, it follows that the observed isotope effect must come from σ_{cap} and not from the survival factor. It may be of interest to note that an isotope dependence $\sigma_{\text{cap}} \propto M^{1/4}$, such as occurs for diatomic molecules, would lead to $\sigma_{\text{DA}}(\text{CD}_4)/\sigma_{\text{DA}}(\text{CH}_4) = 1.2$ in good agreement with the experimental results.

10.6. Dissociative attachment in other molecules

The isotope effect for dissociative attachment in H_2O and D_2O has been studied by Compton and Christophorou (1967), and in the hydrogen halides by Christophorou *et al.* (1968). In both these cases isotope effects with $\sigma_{\text{DA}} \propto M^{-1/2}$ are reported. Theoretically this is difficult to understand but Compton and Christophorou attribute this to non-adiabatic terms.

A survey of dissociative attachment, giving many references, will be found in the review article by Christophorou and Compton (1967). Further such measurements have been reported by Grob (1963), von Trepka and Neuert (1963), Jäger and Henglein (1966) and Wentworth *et al.* (1967).

11. Vibrational excitation

11.1. Theory of vibrational excitation

The resonance mechanism is very important for vibrational excitation of molecules. It can lead to greatly enhanced cross sections and to complex structure in these cross sections which would otherwise be difficult to understand. Both these effects are due to the severe distortion of the target molecule in a resonance process as compared with a direct reaction.

The theory of vibrational excitation has been considered by Herzenberg and Mandl (1962), Chen (1964 a, b) and Bardsley *et al.* (1966 b). In the last paper a general expression is derived for the cross section $\sigma(\mu \rightarrow \nu)$ for the excitation from the initial vibrational state $\zeta_\mu(R)$ to the final vibrational state $\zeta_\nu(R)$. In discussing vibrational excitation we shall assume that at a given energy only one electronic resonant state is important. This is the usual situation. In this case the expression for the cross section reduces to

$$\sigma(\mu \rightarrow \nu) = 4\pi \frac{k_\nu}{k_\mu} \left(\frac{M}{m}\right)^2 (N+1)^2 \frac{2S_\mu + 1}{2(2S_\mu + 1)} \sum |I_{\nu\mu}^n|^2 \quad (11.1)$$

where the summations are over the orbital angular momentum quantum numbers, and their z components, of the incident and scattered electron. $I_{\nu\mu}^n$ is given by

$$I_{\nu\mu}^n \equiv \int_0^\infty dR \int_0^\infty dR' \zeta_\nu(R) \frac{\phi_\nu^n(r_0, R)}{k_\nu h_\nu^+(k_\nu r_0)} G_n(R, R') \zeta_\mu(R') \frac{\phi_\mu^n(r_0, R')}{k_\mu h_\mu^+(k_\mu r_0)}. \quad (11.2)$$

Equations (11.1)–(11.2) follow from the scattered wave Ψ_{so} , equation (9.9), by projecting out a particular final vibrational state ζ_ν , except that we have here inserted the spin and other factors which would result from a fully antisymmetrized theory.

A general procedure for evaluating the cross section (11.1)–(11.2) is to use the expression (9.15) for the Green function. This form is particularly useful if vibrational excitation occurs in competition with dissociative attachment, i.e. if $E > E_n(\infty)$ (or other dissociative reactions such as $e + AB \rightarrow e + A + B$). This case is illustrated in figure 16(a), but the resonant potential $E_n(R)$ could equally be purely repulsive. The magnitude of the vibrational excitation cross section and its variation with energy depend on the lifetime \hbar/Γ_n of the resonance and on the resonance potential $E_n(R)$ since these determine the probability for re-emission of the electron and the distortion of the residual target molecule.

A very different situation arises for the potential energy curves shown in figure 16(b), where elastic scattering and vibrational excitation are the only open channels and where the resonance potential $E_n(R)$ possesses a minimum. The nuclei can then oscillate in the resonance potential in different vibrational states very much as in a stationary state, provided the lifetime of the complex is long enough. In this case, we use equation (9.17) for the Green function in (11.2). If we assume that $\Gamma_n(R)$ is a slowly varying function for values of R such that $\zeta_\nu(R)$ is appreciable and replace it by a mean value $\bar{\Gamma}_n$, then we can rewrite (11.2) as

$$I_{\nu\mu}^n = \sum_{E'} \frac{b_\nu^n(E') b_\mu^n(E')}{E' - E - \frac{1}{2}i\bar{\Gamma}_n} \quad (11.3)$$

where

$$b_\nu^n(E') \equiv \int_0^\infty dR \frac{\zeta_\nu(R) \phi_\nu^n(r_0, R)}{k_\nu h_\nu^+(k_\nu, r_0)} u_n(E', R). \quad (11.4)$$

This expression can be further simplified since $\phi_\nu^n(r_0, R)$ is a slowly varying function of R . With a suitable mean value \bar{R} we can then write

$$b_\nu^n(E') = \frac{\phi_\nu^n(r_0, \bar{R})}{k_\nu h_\nu^+(k_\nu, r_0)} \int_0^\infty dR \zeta_\nu(R) u_n(E', R). \quad (11.5)$$

The last integral is the usual Franck–Condon factor; it is the overlap integral of the oscillator wave functions in the potential of the target molecule and of the resonance complex.

The vibrational excitation cross sections show very different structure depending, on the one hand, on the relative time scales of the resonance lifetime $\hbar/\bar{\Gamma}_n$ and the vibrational period $1/\omega$ (where $\hbar\omega$ is the vibrational spacing in the resonance potential $E_n(R)$) and, on the other hand, on the strength of the coupling of the extra electron, i.e. on the force which it exerts on the nuclei. This qualitative classification of different régimes was derived by Herzenberg and Mandl (1962), and we shall now discuss the main features.

11.1.1. *Compound-molecule limit.* This situation arises if the lifetime $\hbar/\bar{\Gamma}_n$ of the resonance is very long compared with the vibrational period $1/\omega$ in the resonance potential:

$$\bar{\Gamma}_n \ll \hbar\omega. \quad (11.6)$$

In this case the nuclei perform many oscillations while the extra electron is resident in the complex. This is the compound-molecule limit, so called in analogy with Bohr's compound-nucleus model. As a consequence of (11.6) different vibrational states of the resonance do not interfere but correspond to well-separated poles of the scattering amplitude (11.3). Furthermore, the excitation cross sections for different *final* vibrational states of the target all have peaks at the same energies.

The number of such final states excited and their relative probabilities depend on the distortion of the target potential $E_\mu^N(R)$ due to the projectile electron, i.e. on the relative shift of the minima of the potential curves $E_\mu^N(R)$ and $E_n(R)$ (figure 16(b)) and on their curvatures at the minima. The cases of strong and weak coupling correspond to large and small distortion respectively. In the latter case the oscillator wave functions $u_n(E', R)$ and $\zeta_\nu(R)$ in (11.5) are nearly the same. As a result mainly elastic scattering will occur with only very little vibrational excitation.

If the coupling is strong one deals, in general, with two very different potential energy curves. It follows from (11.3) that transitions will occur via a group of compound-molecule levels E' , for which the Franck-Condon factors (11.5) with the initial vibrational state $\zeta_\mu(R)$ are appreciable, and the transitions will be to those final states $\zeta_\nu(R)$ which have appreciable Franck-Condon overlap integrals with this group of compound molecule states $u_n(E', R)$. Hence a whole group of final states ζ_ν will be excited, and the partial cross sections $\sigma(\mu \rightarrow \nu)$ to *different* channels ν will have peaks for the *same* energies. Each peak corresponds to a particular compound-molecule level, and the spacing of these peaks will just be the level spacing $\hbar\omega$.

11.1.2. *Impulse limit.* We now consider the opposite limit

$$\bar{\Gamma}_n \gg \hbar\omega. \quad (11.7)$$

In this case the projectile electron hardly stays in the molecule at all. It just gives a knock to the nuclei, but the nuclei will hardly have moved during the lifetime of the negative ion. Hence this is called the impulse limit. Equation (11.3) still holds but is not the most apt expression. It does not display the essential features; different resonances now overlap and the peaks in different excitation cross-sections occur at *different* energies. One can obtain a more suitable approximate analytic expression by solving the nuclear wave equation (9.12) in time-dependent form, neglecting the time dependence of the perturbing potential, due to the projectile electron, during the short lifetime of the resonance. In this way one finds that

$$\sigma(\mu \rightarrow \nu) \propto \frac{k_\nu}{k_\mu} \left| \int dR \zeta_\nu(R) \frac{1}{E - \epsilon_\nu - \{E_n(R) - E_\mu^N(R)\} + \frac{1}{2}i\Gamma_n(R)} \zeta_\mu(R) \right|^2 \quad (11.8)$$

where we have omitted the electronic matrix element and constant factors.

In deriving equation (11.8) the use of the impulse approximation amounted to omitting the exponential factors from the time-dependent perturbation

$$\exp\left(\frac{iH_0 t}{\hbar}\right) \{W_n(R) - E_\mu^N(R)\} \exp\left(\frac{-iH_0 t}{\hbar}\right) \quad (11.9)$$

where

$$H_0 \equiv H_N + E_\mu^N(R). \quad (11.10)$$

This is justified provided the R dependence of the perturbing potential

$$W_n(R) - E_\mu^N(R)$$

is mainly linear, for values of R that matter, with only small contributions from higher powers of $R - R_0$. In this case the dominating time dependence of (11.9) will be of the form $\exp(\pm i\omega_0 t)$, where ω_0 is the vibrational frequency in the ground-state potential $E_\mu^N(R)$. In the impulse limit the lifetime of the resonance, \hbar/Γ_n , will be small compared with $1/\omega_0$ so that the exponentials in (11.9) may be replaced by unity. The detailed derivation of a somewhat more restrictive form of (11.8) is given by Herzberg and Mandl (1962).

Limiting situations of weak and strong coupling occur, depending on whether the variation of $E_n(R) - E_\mu^N(R)$ within the Franck-Condon region $|R - R_0| \leq a$ (to which the nuclear ground-state wave function ζ_μ restricts the integration in (11.8)) is small or large compared with $\Gamma_n(R)$ in that region. More precisely, with

$$\alpha(R) \equiv \frac{2av_1(R)}{\Gamma_n(R)} \equiv \frac{2a}{\Gamma_n(R)} \frac{\{E_n(R) - E_\mu^N(R)\} - \{E_n(R_0) - E_\mu^N(R_0)\}}{R - R_0} \quad (11.11)$$

weak and strong coupling are defined by $\alpha(R) \ll 1$ and $\alpha(R) \gg 1$ for $|R - R_0| \leq a$. This interpretation results from the fact that $\alpha(R)$ is the ratio of $v_1(R)\hbar/\Gamma_n(R)$, the momentum transferred to the nuclei by the projectile in the collision, divided by $\hbar/2a$, the momentum of the nuclear motion in the initial state ζ_μ .

For these limiting cases we can obtain approximate expressions for $\sigma(\mu \rightarrow \nu)$. For weak coupling we expand (11.8) in powers of α . If, for simplicity, we take $\Gamma_n(R) = \Gamma_n(R_0)$ and make the linear approximation $v_1(R) = v_1(R_0)$ within the Franck-Condon region, the main contribution to (11.8) comes from $\{\alpha(R_0)\}^\nu$. The partial cross section $\sigma(\mu \rightarrow \nu)$ then has a single peak which occurs at energy $E = E_\nu \equiv \epsilon_\nu + E_n(R_0) - E_\mu^N(R_0)$, i.e. the peak moves to higher energies as ν increases. The peak cross section is proportional to $\{\alpha(R_0)\}^{2\nu}$. Thus there will be mainly elastic scattering with the excitation cross sections $\sigma(\mu \rightarrow \nu)$ decreasing rapidly as the vibrational quantum number ν increases.

In the opposite limit of strong coupling a rather drastic approximation leads to

$$\sigma(\mu \rightarrow \nu) \propto \frac{k_\nu}{k_\mu} \left| \zeta_\nu \left\{ R_0 + \frac{E - E_\nu}{v_1(R_0)} \right\} \zeta_\mu \left\{ R_0 + \frac{E - E_\nu}{v_1(R_0)} \right\} \right|^2. \quad (11.12)$$

It follows that many vibrational levels will be excited. On account of the oscillatory nature of the vibrational wave functions ζ_μ, ζ_ν the partial cross sections $\sigma(\mu \rightarrow \nu)$ will possess many peaks which occur at different energies for different channels ν (for details regarding these limiting cases, see Herzberg and Mandl (1962)).

11.2. Elastic scattering

In §11.1 we considered electron scattering which occurs via a resonance. In addition the scattering amplitudes will contain a non-resonant component. These two components will have different angular distributions and energy dependences and will interfere with each other. Now inelastic processes result from a severe

distortion of the target and will therefore primarily occur via resonances which represent such a distortion. The elastic scattering will, of course, also display some structure due to resonances but, since it will in general also contain a large non-resonant component, it is much harder to analyse. Hence inelastic processes are particularly useful for studying resonances.

In the remainder of this section we shall give examples of electron-molecule scattering where resonances produce structure and where many of the characteristic features discussed in § 11.1 show up.

11.3. Vibrational excitation of H_2 at low energies

Measurements of the energy dependence of the vibrational excitation cross sections of H_2 in the energy range up to about 8 eV have been reported by Engelhardt and Phelps (1963), Schulz (1964) and Erhardt *et al.* (1968). Figure 21 shows the results of the first two groups of authors† and compares them with the calculations

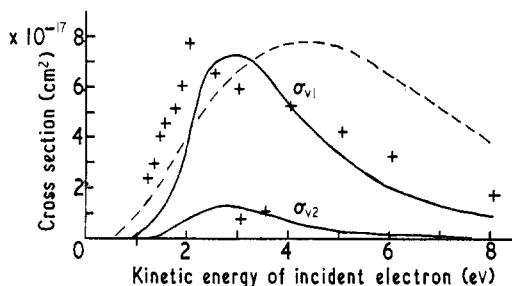


Figure 21. Cross sections for the excitation of the two lowest vibrational states of H_2 by electron impact. Broken curve, Engelhardt and Phelps 1963; crosses, Schulz 1964 (multiplied by 1.4); full curves, calculations of Bardsley *et al.* (1966 b). (From Bardsley *et al.* 1966 b.)

of Bardsley *et al.* (1966 b) for vibrational excitation via the $2\Sigma_u^+$ resonance of H_2^- discussed in § 3.1. The agreement is seen to be good. These cross sections are a factor 15 to 30 larger than ones calculated by Born approximation (Carson 1954). On the other hand, Takayanagi (1965), using a distorted wave approximation, obtains the right order of magnitude for the $v = 1$ excitation cross section. This is consistent with the description of this H_2^- state as a ground-state shape resonance (see § 3.1), i.e. of an electron retained by a centrifugal barrier in the frozen target ground state.

The cross sections in figure 21 have the features which were described in § 11.1.2 as typical of the impulse limit and weak coupling. This is consistent with the properties of a broad p-wave shape resonance and, in particular, with the resonance parameters which follow from the calculation of Bardsley *et al.* (1966 a) reported in § 3.1: $\Gamma_n(R_0) \simeq 4.5$ eV; $\hbar\omega \simeq 0.2$ eV; $2av_1(R_0)/\Gamma_n(R_0) \simeq \frac{1}{3}$.

† The results of Schulz have been multiplied by a factor 1.4 to correct for the fact that he observed at 70° and assumed s-wave electrons whereas one is dealing with p-wave electrons (see below).

The angular distribution of electrons inelastically scattered in exciting the $v = 1$ vibrational level of H_2 has been measured by Ehrhardt *et al.* (1968) for several incident electron energies in the range 1.0 to 8.0 eV. The angular distributions all have the same shape, shown in figure 22 for incident electrons with an energy of 2.5 eV. This is a typical p-wave distribution as is required on account of the parity

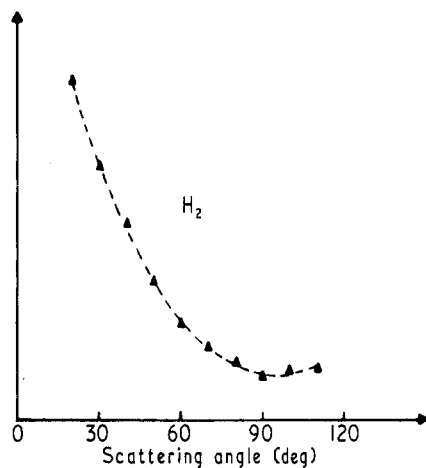


Figure 22. Angular distribution of electrons inelastically scattered in exciting the $v = 1$ vibrational state of H_2 . Energy of incident electrons 2.5 eV. (From Ehrhardt *et al.* 1968.)

and structure of this resonance (see §3.1). They have also measured the elastic angular distributions and these vary strongly with energy in the range 0.8 to 3.4 eV.

11.4. Electron scattering by H_2 near 12 eV

The scattering of electrons in the energy range 11 to 13 eV by H_2 and its isotopes has been measured by several groups of workers (Kuyatt *et al.* 1964, Golden and Bandel 1965, Kuyatt *et al.* 1966, Heideman *et al.* 1966 b, Menendez and Holt 1966). Kuyatt *et al.* (1966) measured the transmitted current from electrons incident on a gas-filled scattering chamber using H_2 , HD and D_2 as targets. They measured the current of electrons transmitted in the forward direction without energy loss as a function of incident electron energy. (Thus peaks in the transmitted current correspond to dips in the total scattering cross section.) In H_2 and HD they observed two series of resonances while in D_2 they found only one series with slight indications of a second series. A typical result for HD is shown in figure 23 while columns 1 to 5 of table 1 show the energies of the observed resonance peaks in H_2 , HD and D_2 , and state the accuracy of these data. The absence of a second resonance series in D_2 is due to the smaller vibrational spacing in D_2 (the spacing is inversely proportional to the square root of the reduced mass) which makes observation harder, and to the fact that in D_2 the two series closely overlap. To check this last point, Kuyatt *et al.* (1966) predict *both* series of resonances in D_2 by scaling the vibrational constants for the H_2 and HD series. The resulting series for D_2 are shown in columns 6 and 7 of table 1 and are seen to have a high overlap.

Heideman *et al.* (1966 b) observed the energy dependence of the excitation cross sections of the $v = 0$ and $v = 1$ vibrational states of the $B^1\Sigma_u^+$ state of H_2 . These

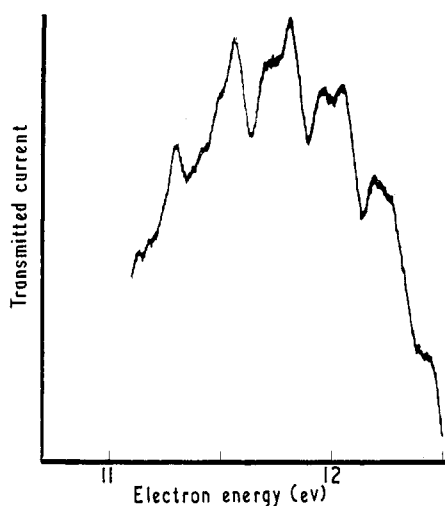


Figure 23. Transmitted current (without energy loss in forward direction) in HD as a function of incident electron energy in eV. (From Kuyatt *et al.* 1966.)

Table 1. The H_2^- , HD^- and D_2^- resonances near 12 eV

Column Series	Observed†				Predicted‡		Calculated§		
	1 H_2 1	2 H_2 2	3 HD 1	4 HD 2	5 D_2 —	6 D_2 1	7 D_2 2	8 H_2 1	9 H_2 2
	11·28		11·28		11·28	11·28		11·07	
		11·46		11·47			11·47		11·46
	11·56		11·54		11·48	11·49		11·37	
		11·72		11·70			11·67		11·75
	11·84		11·79		11·69	11·70		11·66	
		11·99		11·95			11·86		12·03
	12·11		12·02		11·89	11·90		11·93	
		12·27		12·19			12·06		12·31
	12·37		12·27		12·09	12·10		12·19	
		12·53		12·42			12·25		12·58
	12·62		12·49		12·28*	12·29		12·43	
		12·77		12·65*			12·44		12·84
	12·86*				12·47*	12·48		12·65	
		12·97*		12·84*			12·62		13·09
					12·64	12·67			
					12·85	12·85			

† Kuyatt *et al.* 1966. Relative values are estimated to be accurate within 0·01 eV, except those with an asterisk which are estimated to be accurate within 0·02 eV. Absolute values are estimated to be accurate within 0·1 eV.

‡ Obtained by Kuyatt *et al.* (1966) from columns 1 to 4 by scaling the vibrational constants.

§ Eliezer *et al.* 1967.

results are shown in figure 24. The resonance peaks in both these curves occur at the same energies. The spacing of these peaks is the same as that of the transmission peaks observed by Kuyatt *et al.* (1966). Both these facts are typical of the compound-molecule régime, as discussed in § 11.1.1.

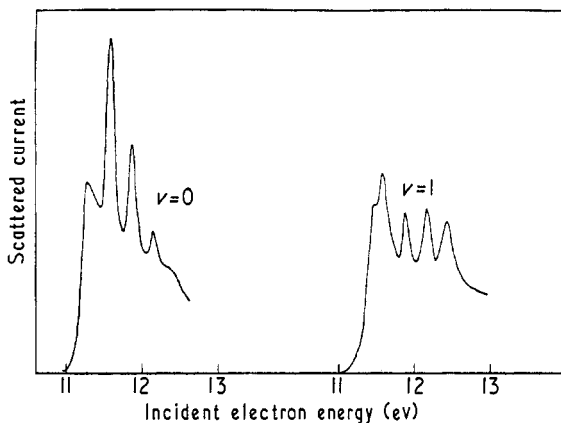


Figure 24. Excitation probability as a function of the incident electron energy for the $v = 0$ and $v = 1$ vibrational levels of the $B\ ^1\Sigma_u^+$ state of H_2 . (From Heideman *et al.* 1966 b.)

The theoretical analysis of these experiments was initiated by Taylor and Williams (1965) and greatly improved by Eliezer *et al.* (1967). The last authors interpreted the two observed series of resonances as the vibrational levels of two core-excited Feshbach resonances of H_2^- , the parent states being the

$$(1s\sigma_g)(2p\pi_u)C\ ^3\Pi_u$$

and

$$(1s\sigma_g)(2p\pi_u)C\ ^1\Pi_u$$

states of H_2 , both resonances being $^2\Sigma_g^+$ states. These resonances were discussed in § 4.3 and their potential energy curves and those of their parent states (lying above them as required) are shown in figure 7. Columns 8 and 9 of table 1 give the vibrational levels of H_2^- in these two resonance potentials as calculated by Eliezer *et al.* The agreement in the level spacings is very good. It is difficult to draw any conclusions about the absolute energies of the resonances since the peaks in the transmitted current do not necessarily coincide with the positions of the resonances. The level spacings of these two resonances are very similar to those of their target states, indicating that the extra electron is moving rather far out in the molecule and thus does not appreciably modify the nuclear potential. Finally we note that the potential energy curves of the two resonant states have very different curvatures and displaced minima relative to the corresponding quantities of the H_2 ground state, showing that we are dealing with a strong coupling situation, as discussed in § 11.1.2 and in agreement with the experimental results of many well-developed cross-section peaks.

11.5. Electron scattering by N_2 near 2 eV

The remarkably complex structure of the cross section for vibrational excitation of N_2 by electrons was first observed by Schulz (1962) whose results for the excitation of the second to eighth vibrational levels, for electrons scattered through 72° , are shown in figure 25. Subsequently, improved and extended energy spectra for elastic and inelastic scattering have been obtained (Schulz 1964, Heideman *et al.* 1966 a, Schulz and Koons 1966, Andrick and Ehrhardt 1966, Golden 1966, Ehrhardt and Willmann 1967).

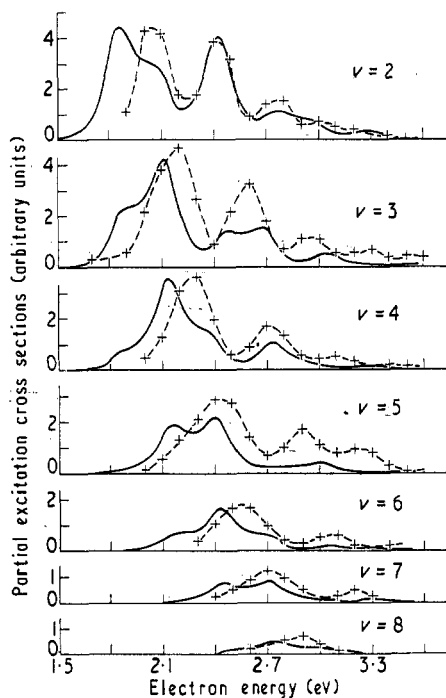


Figure 25. Energy dependence of the cross sections for excitation of the second to eighth vibrational levels of N_2 by electron impact. Crosses and broken curves, Schulz 1962; full curves, Herzenberg and Mandl 1962. The $v = 2$ curves are normalized to give the same magnitude for the first peak. The normalization of the other curves is then determined. All curves are on the same scale. (From Herzenberg and Mandl 1962.)

The first theoretical analysis of Schulz's curves (figure 25) was carried out by Herzenberg and Mandl (1962), who ascribed the observed structure to a resonance which, in the notation of § 11.1, they described by parameters $E_n(R_0)$, $\Gamma_n(R_0)$, $v_1(R_0)$ using the linear approximation to obtain $E_n(R)$ for other internuclear separations. The spacing of the vibrational levels in the resonance they took equal to that of the N_2 ground state, i.e. 0.3 eV. A numerical solution of the nuclear wave equation then gave the vibrational excitation cross sections in terms of these three parameters which were determined by optimizing the fit of these theoretical cross sections to Schulz's results. The optimum theoretical results are shown as full curves in figure 25. Considering the complexity of the data and the fact that the theory

contains only three adjustable parameters, the agreement is extremely good. The optimum values of the parameters are $E_n(R_0) = 2.3$ eV, $v_1(R_0) = 1.2 \times 10^9$ eV cm⁻¹ and $\Gamma_n(R_0) = 0.2$ eV. This is of the same order as the vibrational spacing so that one is in a situation in between the impulse and compound-molecule limits. Nevertheless, the behaviour of the cross sections, shown in figure 25, is reminiscent of the impulse limit. J. N. Bardsley (unpublished), using equations (11.1)–(11.5), greatly improved the agreement with experiment by also varying the level spacing $\hbar\omega$ in the resonance, the best agreement being obtained for $\hbar\omega = 0.22$ eV and

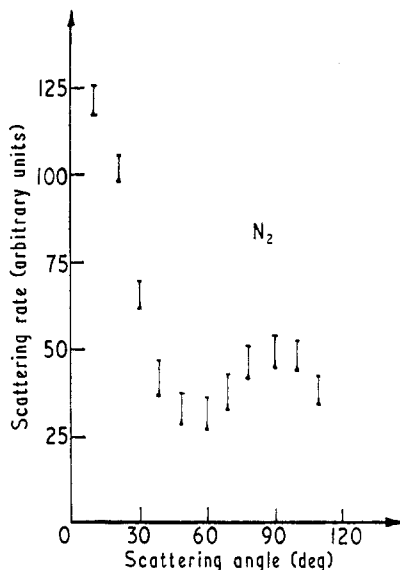


Figure 26. Angular distribution of electrons inelastically scattered in exciting the $v = 1$ vibrational state of N_2 . Incident electron energy, 1.9 eV. (From Ehrhardt and Willmann 1967.)

$\bar{\Gamma}_n = 0.16$ eV. Very similar results were obtained by Chen (1964 b) using $\hbar\omega = 0.24$ eV and $\bar{\Gamma}_n = 0.15$ eV. Chen has improved the agreement between theory and experiment further by allowing for anharmonicity effects (Chen 1964 c). He has also considered the systematic variation of the Franck–Condon factors (Chen 1966 c) and rotational excitation via a resonance (Chen 1966 a).

Ehrhardt and Willmann (1967) have measured the angular distribution in the range 0 to 110° for both elastic and inelastic scattering of electrons by N_2 , for various incident electron energies in the range 1.4 to 3.9 eV. In the inelastic scattering they report angular distributions for the excitation of the vibrational levels $v = 1, 3$ and 5. The elastic angular distributions are difficult to analyse because of the large non-resonant component which they manifestly contain. (This shows up particularly well in the energy dependence of the elastic cross sections at fixed angles measured by Andrick and Ehrhardt (1966) and by Ehrhardt and Willmann (1967).) Over the range 1.4 to 3.9 eV the elastic angular distribution varies drastically. In contrast, the angular distribution of the inelastic cross sections shows the same general shape for the observed energy range 1.9 to 3.1 eV and vibrational states $v = 1, 3, 5$. This is the behaviour expected from scattering via a resonance. The angular distribution

is largely determined by the structure of the resonance. A typical result of Ehrhardt and Willmann is shown in figure 26 which gives the angular distribution at 1.9 eV for the excitation of the $v = 1$ level. This angular distribution is consistent with a ${}^2\Pi_g$ resonance, as discussed in §3.2. For such a resonance the extra electron must be in a π_g state, i.e. it must have even orbital angular momentum l with projection on to the molecular axis of one unit of angular momentum, i.e. we require $l \geq 2$. The simplest such angular distribution for $l = 2$ which one would expect to be adequate for a simple structure such as a ground-state shape resonance is in agreement with the results of Ehrhardt and Willmann (for details, see Bardsley *et al.* 1967). As discussed in §3.2, a d-wave resonance produces a quite effective centrifugal barrier which may lead to a comparatively narrow resonance. The width of 0.15 to 0.20 eV determined from the energy dependence of the inelastic scattering is consistent with this interpretation.

The energy and angular dependences of the vibrational excitation cross sections of CO near 2 eV have also been measured (Schulz 1964, Ehrhardt *et al.* 1968). The energy dependence is similar to that for N_2 but corresponds to a somewhat larger width. The angular distribution is predominantly that of p-wave electrons (although some d-wave contributions are to be expected and are observed). Both these features follow from the fact, discussed in §3.3, that g-u symmetry does not hold for CO. Consequently, emission of p-wave electrons is possible. Because of the lower centrifugal barrier, compared with d waves, this also results in a larger width.

12. Non-adiabatic collision processes

In this section we shall examine the consequences of the breakdown of the Born-Oppenheimer approximation. The most important effect is the existence of nuclear-excited Feshbach resonances, and the treatment of two classes of such resonances will be described in §§12.1 and 12.2. For the other two types of resonances the non-adiabatic effects will in general be small. Exceptions to this may be found in the collisions of thermal electrons with molecules (Bardsley 1968 a). Compton and Christophorou (1967) have also suggested that these effects may be important in dissociative attachment in water and the hydrogen halides.

12.1. *Vibrationally excited Rydberg states*

The excited vibrational levels of the Rydberg states of molecules often lie above the ground-state energy of the corresponding positive ion. In this situation the states can autoionize through the exchange of energy between electronic and nuclear motion in the manner described in §2.3. This autoionization process can be described in perturbation theory using the Born-Oppenheimer solutions as zero-order wave functions (Berry 1966, Bardsley 1967 b). The Rydberg states are represented by a product of an electronic wave function Ψ_n^i and a nuclear function ζ_n^i . The final state in the decay process, representing an electron being emitted, leaving a molecular positive ion, is written as a similar product $\Psi_v^f \zeta_v^f$.

The perturbation causing the transition arises from those terms in the Hamiltonian which are neglected in the Born-Oppenheimer approximation; that is, they are the terms coming from the application of the nuclear kinetic energy

operator to the electronic wave function. Thus the matrix element which governs the transition is

$$V_{nv} = -\frac{\hbar^2}{M} \langle \Psi_\nu^f \zeta_\nu^f | \nabla_{\mathbf{R}} \Psi_n^i \cdot \nabla_{\mathbf{R}} \zeta_n^i \rangle - \frac{\hbar^2}{2M} \langle \Psi_\nu^f \zeta_\nu^f | \zeta_\nu^i \nabla_{\mathbf{R}}^2 \Psi_n^i \rangle. \quad (12.1)$$

This description is analogous to the configuration interaction approach (Dibeler *et al.* 1965). The resonant width is expressed in terms of this matrix element as $2\pi |V_{nv}|^2$.

The matrix elements V_{nv} have been studied by Berry (1966) and Bardsley (1967 b). They conclude that autoionization occurs most readily when transitions are possible which involve a change Δv in vibrational quantum number of unity. The autoionization rate decreases rapidly with increasing values of Δv . Bardsley shows that for a given value of Δv the rate decreases with increasing value of the principal quantum number of the Rydberg state. If the effective principal quantum number is n^* (so that the binding energy is $\frac{1}{2}(n^*)^{-2}$ A.U.), the decay rate varies approximately as $(n^*)^{-3}$.

Berry and Bardsley were mostly concerned with the Rydberg states formed by photon impact upon hydrogen molecules. In this case the outermost electron of the Rydberg state will normally have orbital angular momentum l of unity. Russek *et al.* (1968) have examined the dependence of the autoionization rate upon l . They show that the lifetimes of states with $l = 0$ should be much longer than those with $l = 1$. In H_2 and HD they calculate the lifetimes of some typical states with $l = 0$ to be between 10^{-6} and 10^{-9} s. Barnett and Ray (1968) have observed neutral molecules in beams of H_2^+ , HD^+ and D_2^+ , and Russek *et al.* attribute these to Rydberg states with $l = 0$ which are formed in collisions with electrons.

12.2. Long-lived resonances in polyatomic molecules

Compton *et al.* (1966 b) have measured the lifetimes of nuclear-excited Feshbach resonances in large molecules and their results are of the order of microseconds (see § 5.3). They give a simple model for the interpretation of their results.

They relate the lifetime τ of the negative ion to the capture cross section σ_c through the principle of detailed balance:

$$\tau = \frac{\rho^-}{\rho^0} \frac{1}{v \sigma_c}$$

where ρ^- is the density of states of the negative ion, ρ^0 the product of the density of states for the incident electron and the neutral molecule, and v is the velocity of the incident electron. From this expression one can see that the existence of a large density ρ^- of negative ion states will lead to a long lifetime. This density of states is determined by the amount of energy available for the nuclear motion of the molecule. This energy is the sum of the energy of the incident electron, the electron affinity and the zero-point vibrational energy of the negative ion (Rabinowitz and Diesen 1959).

Thus the resonant lifetime can be expressed in terms of the molecular electron affinity. Compton *et al.* use this fact to deduce values for the electron affinities from the measured lifetimes and capture cross sections. They obtain the values 0.4 eV

for $C_6H_5NO_2^-$, 1.1 eV for $(CH_3CO)_2^-$ and 1.1 eV or 1.4 eV for SF_6^- , depending on which of two possible sets of experimental results is used. From their comments and from the discussion of Klots (1967) it is clear that the electron affinities obtained from this simple treatment are at best lower limits and should not be taken too seriously. Nevertheless, their calculations show that lifetimes of the order of microseconds are reasonable for nuclear-excited Feshbach resonances in such complex molecules.

13. Heavy particle collisions

The complete discussion of the resonances which occur in the collisions of atoms and molecules with each other is not within the scope of this article. We have concentrated our attention on resonant states which decay by electron emission, and so our main purpose in this section will be to discuss the role of these resonances in atom-atom and atom-molecule collisions. However, since our classification of resonances may be useful in the more general context we shall briefly discuss resonant states which are stable against electron emission in § 13.4.

We shall restrict our attention mainly to atom-atom collisions. We shall consider such collisions at energies up to a few keV, for which the perturbed stationary state approach can be used (Massey and Smith 1933, Bates *et al.* 1953, Bates 1962). The method is based on the suggestion of Mott (1931) that the wave function of the scattering system should be expanded in terms of the electronic states of the molecule which is formed by the colliding atoms. The success of the method is due to the fact that often only a few terms need be retained in this expansion.

One difficulty which arises in the application of this method can be illustrated by the example of $H-H^-$ collisions. For the molecule H_2^- at small internuclear distances there are no bound states. Hence, if one used only bound electronic states in the expansion, then the method could not be applied to these collisions. The solution is clearly that one should include both bound and resonant states in the expansion. This procedure will be illustrated in §§ 13.1 to 13.3.

13.1. Electron detachment in $H-H^-$ collisions

The incorporation of resonant states within the perturbed-stationary-state approach greatly facilitates the calculation of electron detachment cross sections. We shall briefly describe the calculation following the method used by Bardsley (1967 a) and Dalgarno and Browne (1967). Very similar methods have been used by Chen (1967) and Herzenberg (1967).

The motion of the two nuclei can be reduced effectively to one dimension by the assumption that they move along classical trajectories. The detachment cross section is then calculated in two stages. First, for each orbit the probability of detachment is calculated, and then the result is integrated over all possible orbits.†

We include in the expansion of the wave function only the two states of H_2^- which for large R lead to the ground states of H and H^- . These are the $^2\Sigma_u^+$ resonance discussed in § 3.1 and the $^2\Sigma_g^+$ resonance of § 6.1. The electronic wave

† For an alternative approach in terms of a partial wave analysis see Herzenberg (1967).

functions for these two states will be denoted by $\chi^\pm(q, \mathbf{R})$ where q denotes the coordinates of all three electrons. The plus and minus signs distinguish the two states according to their parity. Their potential energy curves and resonant widths will be denoted by $E^\pm(R)$ and $\Gamma^\pm(R)$. The wave function representing the collision can then be written

$$\Psi(q, t) = c^+(t)\chi^+(q, \mathbf{R}(t)) + c^-(t)\chi^-(q, \mathbf{R}(t)). \quad (13.1)$$

Before the collision the coefficients $c^\pm(t)$ are equal in both amplitude and phase. After the collision the coefficients will be reduced in amplitude because of electron detachment and will be out of phase because of the difference in the two potentials $E^\pm(R)$. The difference in phase affects the charge-transfer cross sections (Bardsley 1967 a) but the detachment cross section is determined by the reduction in amplitude. For an orbit with impact parameter p the probability of electron detachment is then

$$\begin{aligned} P_{\text{ED}}(p) &= 1 - \left| \frac{c^+(+\infty)}{c^+(-\infty)} \right|^2 - \left| \frac{c^- (+\infty)}{c^- (-\infty)} \right|^2 \\ &= 1 - \frac{1}{2} \exp\{-2\gamma^+(p)\} - \frac{1}{2} \exp\{-2\gamma^-(p)\} \end{aligned} \quad (13.2)$$

in which

$$\begin{aligned} \gamma^\pm(p) &= \frac{1}{2\hbar} \int_{-\infty}^{+\infty} \Gamma^\pm(R(t)) dt \\ &= \frac{1}{\hbar} \int_{R_{c^\pm}}^{\infty} \frac{\Gamma^\pm(R)}{dR/dt} dR. \end{aligned} \quad (13.3)$$

From conservation of energy and angular momentum one finds that

$$\frac{dR}{dt} = \left[\frac{2E}{M} \left\{ 1 - \frac{p^2}{R^2} - \frac{E^\pm(R) - E^\pm(\infty)}{E} \right\} \right]^{1/2}. \quad (13.4)$$

E is the relative scattering energy, M the reduced mass and R_{c^\pm} is the distance of closest approach. In terms of this probability the cross section for electron detachment is

$$\sigma_{\text{ED}} = 2\pi \int_0^\infty P_{\text{ED}}(p) p dp. \quad (13.5)$$

At energies of 50 eV and above the classical trajectory for the nuclear motion can be approximated by a straight line. Using this approximation Bardsley (1967 a) calculated the electron detachment cross sections using the H_2^- potential curves and resonant widths of Bardsley *et al.* (1966 a). In figure 27 these results are compared with the measurements of Hummer *et al.* (1960).

13.2. Associative detachment in $\text{H}-\text{H}^-$ collisions at thermal energies

In $\text{H}-\text{H}^-$ collisions at energies below 0.7 eV the emission of an electron must be accompanied by the formation of a molecule H_2 . This is of special interest in astrophysics (Lambert and Pagel 1968). At low energies the nuclear motion cannot be assumed to be rectilinear. For impact parameters below a critical value the long-range polarization potential produces a spiralling motion, which greatly enhances the probability of a close collision (Langevin 1905, Gioumousis and Stevenson

1958). If the energy of relative motion is E , then this critical value is $(2\alpha/E)^{1/4}$ where α is the polarizability of the hydrogen atom.

Herzenberg (1967) and Schmeltekopf *et al.* (1967) have shown that the occurrence of spiralling means that a simple estimate of the associative detachment cross section can be made. At thermal energies the only important contributions come from the lowest ${}^2\Sigma_u^+$ and ${}^2\Sigma_g^+$ states of H_2^- . If during collisions at thermal energies

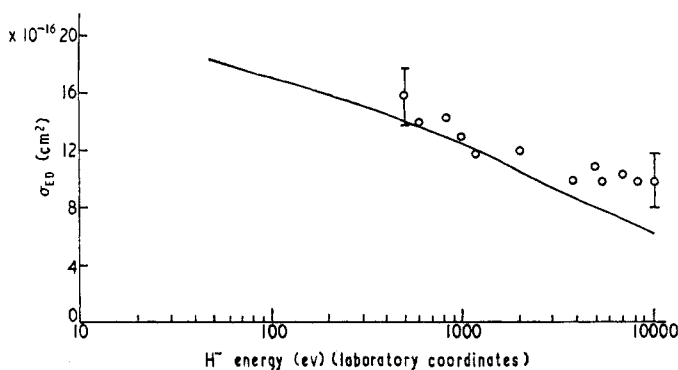


Figure 27. The cross section for electron detachment in $H-H^-$ collisions. Full curve, calculations of Bardsley (1967 a); \circ experimental results of Hummer *et al.* (1960). (From Bardsley 1967 a.)

the electrons take up the ${}^2\Sigma_u^+$ configuration the large width of this state means that electron emission is almost certain to occur if spiralling takes place. The contribution of the ${}^2\Sigma_u^+$ state to the detachment cross section is thus $\frac{1}{2}\pi(2\alpha/E)^{1/2}$. If E is expressed in eV this cross section has the value $7E^{-1/2} \times 10^{-16} \text{ cm}^2$. When averaged over a Maxwell distribution of energies this corresponds to a reaction rate of $1.3 \times 10^{-9} \text{ cm}^3 \text{ s}^{-1}$, independent of the electron temperature.

The contribution of the ${}^2\Sigma_g^+$ state of H_2^- is more difficult to assess until more accurate potential curves are available. It seems probable that its contribution will be small at temperatures below $5000 \text{ }^\circ\text{K}$ so that the reaction rate will be close to $1.3 \times 10^{-9} \text{ cm}^3 \text{ s}^{-1}$ at these temperatures. The rate has been measured by Schmeltekopf *et al.* (1967) who find exactly this value.

The reaction rate for associative detachment in $H-H^-$ collisions has also been calculated by Dalgarno and Browne (1967) who do not use the spiralling approximation but use the theory described in § 13.1 with the H_2^- potential curves and widths of Taylor and Harris (1963) and Bardsley *et al.* (1966 a). They obtain a rate which varies slightly with temperature between $100 \text{ }^\circ\text{K}$ and $32000 \text{ }^\circ\text{K}$ with maximum and minimum values of $1.9 \times 10^{-9} \text{ cm}^3 \text{ s}^{-1}$ and $1.2 \times 10^{-9} \text{ cm}^3 \text{ s}^{-1}$.

Herzenberg (1967) and Chen and Peacher (1968) have studied the distribution of vibrational levels of the molecules formed in associative detachment. They find that the large width of the ${}^2\Sigma_u^+$ state of H_2^- will lead to an inverted population of these levels with most molecules being formed in the highest vibrational states.

Measurements of the rate of associative detachment in other collisions have been reported by Fehsenfeld, Ferguson and Schmeltekopf (1966), Moruzzi and Phelps (1966) and Fehsenfeld *et al.* (1966).

13.3. Ionization in the collisions of two neutral atoms

Large ionization cross sections have been predicted for the process



provided that the reaction is energetically possible and that there is an allowed optical transition between the states A^* and A . This process can be regarded as a consequence of configuration interaction. For each internuclear distance R we can define wave functions to represent the two configurations $A^* + B$ and $A + B^+ + e$ and so we can define the interaction matrix element $V_{fi}(\mathbf{R})$. The autoionization width $\Gamma(\mathbf{R})$ can then be expressed as $2\pi|V_{fi}(\mathbf{R})|^2$ (see § 7.3). The ionization cross section can then be calculated using the approach of § 13.1.

This method has been used by Katsuura (1965), Smirnov and Firsov (1965), Mori (1966), Sheldon (1966) and Watanabe and Katsuura (1967) who all made the following two approximations. The nuclei are assumed to move along straight-line trajectories with a constant relative velocity v . Secondly, the interaction matrix element is represented by the first term in a multipole expansion

$$V_{fi} = \frac{1}{R^3} \left\{ \boldsymbol{\mu} \cdot \boldsymbol{\mu}_{E_0} - 3 \frac{(\mathbf{R} \cdot \boldsymbol{\mu})(\mathbf{R} \cdot \boldsymbol{\mu}_{E_0})}{R^2} \right\} \quad (13.7)$$

(Watanabe and Katsuura 1967). Here $\boldsymbol{\mu}$ is the dipole moment associated with the optical transition $A \rightarrow A^*$, and $\boldsymbol{\mu}_{E_0}$ is the dipole moment associated with the photoionization process $h\nu + B \rightarrow B^+ + e$ in which the photon energy is equal to the excitation energy E_0 of A^* .

Assuming the symmetries $1P$ for A^* , and $1S$ for A , Watanabe and Katsuura show the ionization cross section to be

$$\sigma_i = 13.88 \left(\frac{\mu^2 \mu_{E_0}^2}{\hbar v} \right)^{2/5} \quad (13.8)$$

Katsuura (1965) has previously obtained a similar formula, but with a coefficient of 18.14, by assuming that the dipoles $\boldsymbol{\mu}$ and $\boldsymbol{\mu}_{E_0}$ were always orientated along the internuclear axis. Equation (13.8) leads to a reaction rate

$$\rho = 14.59 \left(\frac{\mu^2 \mu_{E_0}^2}{\hbar} \right)^{2/5} \left(\frac{2kT}{M} \right)^{3/10} \quad (13.9)$$

Values of the reaction rates and cross sections for specific cases have been given by Watanabe and Katsuura (1967) and Sheldon (1966)†.

These reactions may be important in magnetohydrodynamic power generators and in the gas discharges of gas lasers. Therefore it would be worth while to check the approximations involved in this approach. The long-range interactions between the two atoms will cause deviations from the straight-line trajectories and will accelerate the nuclei as they come together. Ferguson (1962) has suggested that spiralling may be important in these collisions and this has not been allowed for in the calculations. Secondly, the effect of the departure of the interaction matrix elements from the asymptotic form (13.7) should be examined. Bates *et al.* (1967) have calculated

† Sheldon uses the cross-section formula of Katsuura (1965) instead of equation (13.8) and so his results should be multiplied by 0.77.

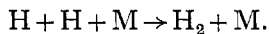
these matrix elements for H-H collisions and find the asymptotic approximation to be valid only for $R > 4$ A.U.

Bates *et al.* (1967) and Bell *et al.* (1968) have calculated the ionization cross sections for collisions involving metastable atoms, for which the approximation (13.7) is not valid. They find that spiralling is very important in such collisions.

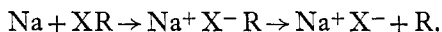
13.4. Electronically stable resonances

It is not essential that resonances occurring in heavy particle collisions should be able to emit electrons. For example, in a collision of two atoms a resonance can occur by the formation of a temporary (but non-autoionizing) diatomic molecule which decays by dissociation. It is also useful to classify these resonances according to the mechanism by which the target and projectile are held together.

Shape resonances can exist in the collisions of any two heavy particles. The shape resonances occurring in H-H collisions have been studied extensively (Bernstein 1966, Bernstein *et al.* 1966, Waech and Bernstein 1967). The positions and widths of these resonances have been computed with high accuracy. The existence of these resonances is due to the combination of the short-range attractive interatomic potential and the centrifugal barrier. In a general discussion of resonances in heavy particle collisions Levine (1967) suggests that these resonances may be important as intermediate states in the three-body recombination process



Electron-excited Feshbach resonances have been discussed in relation to atom-molecule collisions (Wilson and Herschbach 1965, Polanyi 1967). These authors show that the reactions of alkali atoms are of particular interest. For example, in the collision of a sodium atom with a halogen compound there is a large probability that the following reaction will occur



In this reaction the resonant state is formed by a rearrangement of the electronic configuration in which an electron is transferred from the sodium atom to the halogen. Wilson and Herschbach have demonstrated that collisions of electrons and sodium atoms with molecules have many common features. This observation may be of great value in the analysis of resonance formation in atom-molecule collisions.

Nuclear-excited Feshbach resonances may also be important in atom-molecule and molecule-molecule collisions. The resonances in which the kinetic energy of the incident particle is absorbed into the rotational motion of one of the particles have been discussed by Micha (1967) and Levine *et al.* (1968). In both papers model potentials are constructed for atom-molecule collisions and Micha chooses his model parameters to represent the scattering of xenon by H_2 and D_2 . He shows that the rates of formation and decay of the resonances depend mainly on the non-isotropic part of the short-range potential between the target and projectile.

The major goal of the application of resonance theories to heavy particle collisions is an analysis of chemical reactions. The necessary formalism for this has been outlined by Nikitin (1964) and Eu and Ross (1966).

14. Conclusions

One of the most important conclusions to be drawn from this article is that for the understanding of a molecular resonance one requires the results of a fairly comprehensive set of experiments each furnishing its characteristic information. The reason for this is the comparative complexity of molecular resonances due to the interplay of electronic and nuclear motions. Angular distributions provide information about the angular momentum and parity properties of the system. The energy dependence of different vibrational excitation cross sections enables one to determine the lifetime and the coupling strength of a resonance. One needs elastic as well as inelastic data to determine the non-resonant component in the scattering amplitude. The isotope effect in dissociative attachment is invaluable in distinguishing total decay width and capture width, thus providing much information about open and closed channels and about the structure of a resonance.

On the theoretical side one has a reasonable qualitative understanding of the basic features of the simpler resonant collision processes. With the aid of computers it is becoming possible to perform more exact calculations, but processes like dissociative recombination, occurring at thermal energies, present a challenge. There are many outstanding problems about which little is known theoretically. These include situations involving several electronic resonances (the structure observed by Dowell and Sharp (1968) in dissociative attachment in H_2 near 12 eV may be an example of this). The non-adiabatic (i.e. nuclear-velocity dependent) terms deserve more study; they are important in nuclear-excited resonances and may be relevant to the \sqrt{M} -dependent isotope effect reported in dissociative attachment in water and hydrogen halides. Very little work has been done so far on molecular rotations and a generalization of the resonance scattering formalism is required for polyatomic molecules. Finally, one might hope that the study of resonances in heavy particle collisions may lead to a better understanding of chemical reactions.

References

- ALTSHULER, S., 1957, *Phys. Rev.*, **107**, 114–17.
 ANDRICK, D., and EHRHARDT, H., 1966, *Z. Phys.*, **192**, 99–106.
 BARDSLEY, J. N., 1967 a, *Proc. Phys. Soc.*, **91**, 300–5.
 ——— 1967 b, *Chem. Phys. Lett.*, **1**, 229–32.
 ——— 1968 a, *J. Phys. B (Proc. Phys. Soc.)*, [2], **1**, 349–64.
 ——— 1968 b, *J. Phys. B (Proc. Phys. Soc.)*, [2], **1**, 365–80.
 BARDSLEY, J. N., HERZENBERG, A., and MANDL, F., 1964, *Atomic Collision Processes*, Ed. M. R. C. McDowell (Amsterdam: North-Holland), pp. 415–27.
 ——— 1966 a, *Proc. Phys. Soc.*, **89**, 305–19.
 ——— 1966 b, *Proc. Phys. Soc.*, **89**, 321–39.
 BARDSLEY, J. N., MANDL, F., and WOOD, A. R., 1967, *Chem. Phys. Lett.*, **1**, 359–62.
 BARNETT, C. F., and RAY, J. A., 1968, *Phys. Rev.*, in the press.
 BATES, D. R., 1950, *Phys. Rev.*, **78**, 492–3.
 ——— 1962, *Atomic and Molecular Processes* (New York: Academic Press), pp. 549–621.
 BATES, D. R., BELL, K. L., and KINGSTON, A. E., 1967, *Proc. Phys. Soc.*, **91**, 288–99.
 BATES, D. R., MASSEY, H. S. W., and STEWART, A. L., 1953, *Proc. R. Soc. A*, **216**, 437–58.
 BAUER, E., and WU, T.-Y., 1956, *Can. J. Phys.*, **34**, 1436–47.
 BELL, K. L., DALGARNO, A., and KINGSTON, A. E., 1968, *J. Phys. B (Proc. Phys. Soc.)*, [2], **1**, 18–22.

- BERNSTEIN, R. B., 1966, *Phys. Rev. Lett.*, **16**, 385-8.
- BERNSTEIN, R. B., CURTISS, C. F., IMAM-RAHAJOE, S., and WOOD, H. T., 1966, *J. Chem. Phys.*, **44**, 4072-81.
- BERRY, R. S., 1966, *J. Chem. Phys.*, **45**, 1228-45.
- BEUTLER, H., and JUNGER, H.-O., 1936, *Z. Phys.*, **100**, 80-94; **101**, 285-303.
- BLOCH, F., and BRADBURY, N. E., 1935, *Phys. Rev.*, **48**, 689-95.
- BONESS, M. J. W., and HASTED, J. B., 1966, *Phys. Lett.*, **21**, 526-8.
- BONESS, M. J. W., LARKIN, I. W., HASTED, J. B., and MOORE, L., 1967, *Chem. Phys. Lett.*, **1**, 292-4.
- BOWMAN, C. R., and MILLER, W. D., 1965, *J. Chem. Phys.*, **42**, 681-6.
- BURKE, P. G., 1965, *Adv. Phys.*, **14**, 521-68.
- 1968, *J. Phys. B (Proc. Phys. Soc.)*, [2], **1**, 586-8.
- CARSON, T. R., 1954, *Proc. Phys. Soc. A*, **67**, 908-16.
- CHANIN, L. M., PHELPS, A. V., and BIONDI, M. A., 1962, *Phys. Rev.*, **128**, 219-30.
- CHEN, J. C. Y., 1963, *Phys. Rev.*, **129**, 202-10.
- 1964 a, *J. Chem. Phys.*, **40**, 3507-12.
- 1964 b, *J. Chem. Phys.*, **40**, 3513-20.
- 1964 c, *Phys. Lett.*, **8**, 183-4.
- 1966 a, *Phys. Rev.*, **146**, 61-9.
- 1966 b, *Phys. Rev.*, **148**, 66-73.
- 1966 c, *J. Chem. Phys.*, **45**, 2710-12.
- 1967, *Phys. Rev.*, **156**, 12-25.
- CHEN, J. C. Y., and MITTLEMAN, M. H., 1967, *5th Int. Conf. on Atomic Collisions, Abstracts* (Leningrad: Nauka), pp. 329-31.
- CHEN, J. C. Y., and PEACHER, J. L., 1967, *Phys. Rev.*, **163**, 103-11.
- 1968, *Phys. Rev.*, **168**, 56-63.
- CHRISTOPHOROU, L. G., and COMPTON, R. N., 1967, *High Phys.*, **13**, 1277-1305.
- CHRISTOPHOROU, L. G., COMPTON, R. N., and DICKSON, H. W., 1968, *J. Chem. Phys.*, **48**, 1949-55.
- COMPTON, R. N., and CHRISTOPHOROU, L. G., 1967, *Phys. Rev.*, **154**, 110-16.
- COMPTON, R. N., CHRISTOPHOROU, L. G., and HUEBNER, R. H., 1966 a, *Phys. Lett.*, **23**, 656-8.
- COMPTON, R. N., CHRISTOPHOROU, L. G., HURST, G. S., and REINHARDT, P. W., 1966 b, *J. Chem. Phys.*, **45**, 4634-9.
- CRAWFORD, O. H., 1967, *J. Chem. Phys.*, **47**, 1100-4.
- CRAWFORD, O. H., DALGARNO, A., and HAYS, P. B., 1967, *Molec. Phys.*, **13**, 181-92.
- DALGARNO, A., and BROWNE, J. C., 1967, *Astrophys. J.*, **149**, 231-2.
- DANILOV, A. D., and IVANOV-KHOLODNYI, G. S., 1965, *Sov. Phys.-Uspekhi*, **8**, 92-116.
- DEMCOV, Y. N., 1965, *Phys. Lett.*, **15**, 235-6.
- DIBELER, V. H., REESE, R. M., and KRAUSS, M., 1965, *J. Chem. Phys.*, **42**, 2045-8.
- DOWELL, J. T., and SHARP, T. E., 1968, *Phys. Rev.*, **167**, 124-7.
- DUBROVSKY, G. V., OB'EDKOV, V. D., and JANEV, R. K., 1967, *5th Int. Conf. on Atomic Collisions, Abstracts* (Leningrad: Nauka), pp. 342-5.
- EHRHARDT, H., LANGHANS, L., LINDER, F., and TAYLOR, H. S., 1968, *Z. Phys.*, in the press.
- EHRHARDT, H., and WILLMANN, K., 1967, *Z. Phys.*, **204**, 462-73.
- ELIEZER, I., TAYLOR, H. S., and WILLIAMS, J. K., 1967, *J. Chem. Phys.*, **47**, 2165-77.
- ENGELHARDT, A. G., and PHELPS, A. V., 1963, *Phys. Rev.*, **131**, 2115-28.
- EU, B. C., and ROSS, J., 1966, *J. Chem. Phys.*, **44**, 2467-75.
- FANO, U., 1935, *Nuovo Cim.*, **12**, 154-61.
- 1961, *Phys. Rev.*, **124**, 1866-78.
- FEHSENFELD, F. C., FERGUSON, E. E., and SCHMELTEKOFF, A. L., 1966, *J. Chem. Phys.*, **45**, 1844-5.
- FEHSENFELD, F. C., *et al.*, 1966, *Bull. Am. Phys. Soc.*, **11**, 505-6.
- FERGUSON, E. E., 1962, *Phys. Rev.*, **128**, 210-12.
- FESHBACH, H., 1958, *Ann. Phys., N.Y.*, **5**, 357-90.
- 1962, *Ann. Phys., N.Y.*, **19**, 287-313.

- FITE, W. L., and BRACKMANN, R. T., 1963, *Proc. 6th Int. Conf. on Ionization Phenomena in Gases*, Vol. 1 (Paris: S.E.R.M.A.), pp. 21-6.
- FITE, W. L., BRACKMANN, R. T., and HENDERSON, W. R., 1965, *Proc. 4th Int. Conf. on the Physics of Electronic and Atomic Collisions* (New York: Science Bookcrafters), pp. 100-3.
- GILMORE, F. R., 1965, *J. Quant. Spectrosc. Radiat. Trans.*, **5**, 369-89.
- GIOUMOUSIS, G., and STEVENSON, D. P., 1958, *J. Chem. Phys.*, **29**, 294-9.
- GOLDEN, D. E., 1966, *Phys. Rev. Lett.*, **17**, 847-8.
- GOLDEN, D. E., and BANDEL, H. W., 1965, *Phys. Rev. Lett.*, **14**, 1010-13.
- GROB, V. E., 1963, *J. Chem. Phys.*, **39**, 972-8.
- GUNTON, R. C., and SHAW, T. M., 1965, *Phys. Rev.*, **140**, A756-63.
- HAHN, Y., O'MALLEY, T. F., and SPRUCH, L., 1964, *Phys. Rev.*, **134**, B911-19.
- HEIDEMAN, H. G. M., KUYATT, C. E., and CHAMBERLAIN, G. E., 1966 a, *J. Chem. Phys.*, **44**, 355-8.
- 1966 b, *J. Chem. Phys.*, **44**, 440-1.
- HERZBERG, G., 1966, *Electronic Spectra of Polyatomic Molecules* (Princeton, N.J.: Van Nostrand).
- HERZENBERG, A., 1967, *Phys. Rev.*, **160**, 80-94.
- HERZENBERG, A., KWOK, K. L., and MANDL, F., 1964, *Proc. Phys. Soc.*, **84**, 477-97.
- HERZENBERG, A., and MANDL, F., 1962, *Proc. R. Soc. A*, **270**, 48-71.
- 1963, *Proc. R. Soc. A*, **274**, 253-66.
- HUMBLET, J., and ROSENFELD, L., 1961, *Nucl. Phys.*, **26**, 529-78.
- HUMMER, D. G., STEBBINGS, R. F., FITE, W. L., and BRANSCOMB, L. M., 1960, *Phys. Rev.*, **119**, 668-70.
- JÄGER, K., and HENGLEIN, A., 1966, *Z. Naturf.*, **21A**, 1251-9.
- KAPUR, P. L., and PEIERLS, R. E., 1938, *Proc. R. Soc. A*, **166**, 277-95.
- KATSUURA, K., 1965, *J. Chem. Phys.*, **42**, 3771-5.
- KHVOSTENKO, N. I., and DUKEL'SKII, V. M., 1957, *Zh. Eksp. Teor. Fiz.*, **33**, 851-5 (*Sov. Phys.-JETP*, **6**, 657-60 (1958)).
- KLOTS, C. E., 1967, *J. Chem. Phys.*, **46**, 1197-9.
- KUYATT, C. E., MIELCZAREK, S. R., and SIMPSON, J. A., 1964, *Phys. Rev. Lett.*, **12**, 293-5.
- KUYATT, C. E., SIMPSON, J. A., and MIELCZAREK, S. R., 1966, *J. Chem. Phys.*, **44**, 437-9.
- KWOK, K. L., and MANDL, F., 1965, *Proc. Phys. Soc.*, **86**, 501-11.
- LAMBERT, D. L., and PAGEL, B. E. J., 1968, *Mon. Not. R. Astr. Soc.*, in the press.
- LANGVIN, P., 1905, *Ann. Chim. Phys.*, **5**, 245-88.
- LEVINE, R. D., 1967, *J. Chem. Phys.*, **46**, 331-45.
- LEVINE, R. D., JOHNSON, B. R., MUCKERMAN, J. T., and BERNSTEIN, R. B., 1968, *Chem. Phys. Lett.*, **1**, 517-20.
- LEVY-LEBLOND, J. M., 1967, *Phys. Rev.*, **153**, 1-4.
- MACEK, J., and BURKE, P. G., 1967, *Proc. Phys. Soc.*, **92**, 351-64.
- MASSEY, H. S. W., and SMITH, R. A., 1933, *Proc. R. Soc. A*, **142**, 142-72.
- MENENDEZ, M. G., and HOLT, H. K., 1966, *J. Chem. Phys.*, **45**, 2743-4.
- MICHA, D. A., 1967, *Phys. Rev.*, **162**, 88-97.
- MORI, M., 1966, *J. Phys. Soc. Japan*, **21**, 979-86.
- MORUZZI, J. L., and PHELPS, A. V., 1966, *J. Chem. Phys.*, **45**, 4617-27.
- MOTT, N. F., 1931, *Proc. Camb. Phil. Soc.*, **27**, 553-60.
- NIELSEN, S. E., and DAHLER, J. S., 1966, *J. Chem. Phys.*, **45**, 4060-79.
- NIKITIN, E. E., 1964, *Molec. Phys.*, **8**, 473-83.
- O'MALLEY, T. F., 1966, *Phys. Rev.*, **150**, 14-29.
- 1967 a, *Phys. Rev.*, **155**, 59-63.
- 1967 b, *Phys. Rev.*, **156**, 230.
- 1967 c, *Phys. Rev.*, **162**, 98-105.
- OSKAM, H. J., and MITTELSTADT, V. R., 1963, *Phys. Rev.*, **131**, 1578-81.
- PERSSON, K. B., and BROWN, S. C., 1955, *Phys. Rev.*, **100**, 729-33.
- POLANYI, J. C., 1967, *Chem. Phys. Lett.*, **1**, 421-3.
- POPOV, N. A., and AFANASEVA, E. A., 1960, *Sov. Phys.-Tech. Phys.*, **4**, 764-9.
- RABINOWITZ, B. S., and DIESSEN, R. W., 1959, *J. Chem. Phys.*, **30**, 735-47.

- RAPP, D., SHARP, T. E., and BRIGLIA, D. D., 1965, *Phys. Rev. Lett.*, **14**, 533-5.
- RICE, O. K., 1933, *J. Chem. Phys.*, **1**, 375-89.
- RUSSEK, A., PATTERSON, M. R., and BECKER, R. L., 1968, *Phys. Rev.*, **167**, 17-25.
- SCHMELTEKOPF, A. L., FEHSENFELD, F. C., and FERGUSON, E. E., 1967, *Astrophys. J.*, **148**, L155-6.
- SCHULZ, G. J., 1959, *Phys. Rev.*, **113**, 816-19.
- 1962, *Phys. Rev.*, **125**, 229-32.
- 1963, *Phys. Rev. Lett.*, **10**, 104-5.
- 1964, *Phys. Rev.*, **135**, A988-94.
- SCHULZ, G. J., and ASUNDI, R. K., 1965, *Phys. Rev. Lett.*, **15**, 946-9.
- 1967, *Phys. Rev.*, **158**, 25-29.
- SCHULZ, G. J., and KOONS, H. C., 1966, *J. Chem. Phys.*, **44**, 1297-8.
- SHARP, T. E., and DOWELL, J. T., 1967, *J. Chem. Phys.*, **46**, 1530-1.
- SHELDON, J. W., 1966, *J. Appl. Phys.*, **37**, 2928-9.
- SIEGERT, A. F. J., 1939, *Phys. Rev.*, **56**, 750-2.
- SMIRNOV, B. M., and FIRSOV, O. B., 1965, *Sov. Phys.-JETP Lett.*, **2**, 297-300.
- SMITH, K., 1966, *Rep. Prog. Phys.*, **29**, 373-443 (London: Institute of Physics and Physical Society).
- STABLER, R. C., 1963, *Phys. Rev.*, **131**, 1578-81.
- STOCKDALE, J. A. D., CHRISTOPHOROU, L. G., TURNER, J. E., and ANDERSON, V. E., 1967, *Phys. Lett.*, **25A**, 510-11.
- TAKAYANAGI, K., 1965, *J. Phys. Soc. Japan*, **20**, 562-5.
- TAKAYANAGI, K., and ITIKAWA, Y., 1968, *J. Phys. Soc. Japan*, **24**, 160-8.
- TAYLOR, H. S., and HARRIS, F. E., 1963, *J. Chem. Phys.*, **39**, 1012-16.
- TAYLOR, H. S., NAZAROFF, G. V., and GOLEBIEWSKI, A., 1966, *J. Chem. Phys.*, **45**, 2872-88.
- TAYLOR, H. S., and WILLIAMS, J. K., 1965, *J. Chem. Phys.*, **42**, 4063-72.
- VON TREPKA, L., and NEUERT, H., 1963, *Z. Naturf.*, **18A**, 1295-1303.
- TURNER, J. E., 1966, *Phys. Rev.*, **141**, 21-6.
- VAN LINT, V. A. J., WIKNER, E. G., and TRUEBLOOD, D. L., 1960, *Bull. Am. Phys. Soc.*, **5**, 122-3.
- WAECH, T. G., and BERNSTEIN, R. B., 1967, *J. Chem. Phys.*, **46**, 4905-11.
- WATANABE, T., and KATSUURA, K., 1967, *J. Chem. Phys.*, **47**, 800-11.
- WENTWORTH, W., BECKER, R., and TUNG, R., 1967, *J. Phys. Chem.*, **71**, 1652-65.
- WILKINS, R. L., 1966, *J. Chem. Phys.*, **44**, 1884-8.
- WILSON, K. R., and HERSCHBACH, D. R., 1965, *Nature, Lond.*, **208**, 182-3.
- YOUNG, R. A., and ST. JOHN, G., 1966, *Phys. Rev.*, **152**, 25-9.